Distribution of Venus-Expressing Neurons in CRF-Venus Knock-in Mouse Brain and the Effects of Glucocorticoid on Venus Expression in the Paraventricular Nucleus of the Hypothalamus

Distribution of Venus-Expressing Neurons in *CRF-Venus* Knock-in Mouse Brain and the Effects of Glucocorticoid on Venus Expression in the Paraventricular Nucleus of the Hypothalamus

Dissertation

To obtain the Ph.D. degree

Submitted by

Ashraf Hossain Talukder

B1ID2501

Supervised by

Professor Keiichi Itoi

Laboratory of Information Biology

Department of System Information Sciences

Graduate School of Information Sciences

Tohoku University

Sendai, Japan

August, 2014.

Abstract

Corticotropin-releasing factor (CRF) is a key player in the regulation of the hypothalamic-pituitary-adrenal axis. CRF neurons cannot be distinguished morphologically from other neuroendocrine neurons in the paraventricular nucleus of the hypothalamus (PVH) without immunostaining. Thus a knock-in mouse (*CRF-Venus*) was generated by Itoi and colleagues by inserting Venus (enhanced yellow fluorescent protein) gene at the translation initiation site of the CRF gene by homologous recombination, and yet, its expression is driven by the CRF promoter and responds to changes in *milieu interieur*. In the present study, I examined the distribution of Venus-expressing neurons all through the mouse brain including the PVH and compared it with that of CRF expression. In the *CRF-Venus*, Venus-expressing neurons were distributed in brain regions harboring CRF neurons, including the paraventricular nucleus of the hypothalamus (PVH). In the PVH, Venus was expressed selectively in CRF neurons, but a considerable proportion of Venus neurons did not express CRF in a physiological glucocorticoid (GC) state. Following GC deprivation, Venus expression and CRF expression were enhanced in the PVH, and most Venus neurons became expressing of CRF. Conversely, expression of Venus and CRF was suppressed by excess GC. In PVH-Venus neurons, expression of copeptin, a peptide coded within the vasopressin gene, was induced by deprivation of GC, which was suppressed by GC administration. Thus, Venus neurons recapitulated partly the GC-dependent responses of PVH-CRF neurons. This mouse line carried PGK-neo sequence flanking with frt sequence as a positive selection marker for homologous recombination. To examine whether the PGK promoter may have influenced the Venus expression in CRF neurons, another mouse line, *CRF-VenusΔneo was* generated by breeding *CRF-Venus* with *Actb-Flp Knock-in* mouse, and thereby the PGK-neo sequence was deleted from the genomic sequence of the *CRF-Venus* mouse. In the *CRF-VenusΔneo*, Venus was expressed more prominently throughout the brain, and in the PVH, it was expressed more constitutively and most of the Venus-expressing neurons co-localized with CRF in a physiological GC state. With an identical strategy that was used for generating the *CRF-Venus*, *CRF-iCre* knock-in mouse was generated. By crossing *CRF-iCre* with a *CAG-CAT-EGFP* reporter, in which the CAT is floxed, $Tg^{CAG\text{-}CAT\text{-}EGFP/wt}$;$CRF^{iCre/wt}$ (*EGFP/CRF-iCre*) mouse was obtained. EGFP was expressed more constitutively in PVH-CRF neurons of the *EGFP/CRF-iCre* mouse. The mouse models, presented in the present study, will be of great benefit for unraveling the physiological regulatory mechanisms of CRF neurons.

Abbreviations

ACTH	Adrenocorticotropic hormone
ADX	Bilateral adrenalectomy
AVP	Vasopressin
B	Corticosterone
BAC	Bacterial artificial chromosome
CAG promoter	Modified chicken β-actin promoter with CMV-IE enhancer
CAT	Chloramphenicol acetyltransferase
CRF	Corticotropin-releasing factor
EGFP	Enhanced green fluorescent protein
ES	Embryonic stem
FRT	Flp recognition target
GABA	γ–aminobutyric acid
GC	Glucocorticoid
GR	Glucocorticoid receptor
HPA	Hypothalamic pituitary adrenal
i.c.v	Intracerebroventricularly
i.p	Intraperitoneal
NA	Noradrenaline
Neo	Neomycin phosphotransferase
OXT	Oxytocin
PBS	Phosphate buffered saline
Pgk promoter	Phosphoglycerate kinase promoter
PVH	Paraventricular nucleus of the hypothalamus
SRIF	Somatostatin
TRH	Thyrotropin-releasing hormone

Contents

Introduction

The hypothalamus is the integrating center for stress responses [1] and the major neuroendocrine response to stress is via activation of the hypothalamic pituitary adrenal (HPA) axis, consisting of parvocellular neurons in the paraventricular nucleus of hypothalamus (PVH) and consequent release of the neuropeptides, corticotrophin releasing factor(CRF) and arginine vasopressin (AVP), which stimulate pituitary adrenocorticotropic hormone (ACTH) release. This leads to stimulation of glucocorticoid secretion by the adrenal cortex, which is essential for stress adaptation. Glucocorticoids (cortisol in humans and corticosterone in rats and mice) act upon specific receptors present in most peripheral tissues and in the brain, initiating metabolic and neuromodulatory changes necessary for coping with the challenge and CRF and AVP neurons convert stress signals to hormonal outputs [2].

Corticotropin-releasing factor (CRF) is a 41 amino acid peptide that is synthesized in multiple brain regions. In the cortical mantle and basal telencephalon, CRF neurons are usually expressed in the olfactory tubercle, nucleus accumbens, lateral septum, and medial preoptic area, bed nucleus of stria terminalis and in the central nucleus of amygdala. In the cerebral cortex, CRF interneurons are contained in the second and third layers and project to layers I and IV. The highest density of CRF containing neurons is found in the prefrontal, insular and cingulate cortex. In addition with PVH, the CRF neurons also expressed other different parts of diencephalon such as lateral hypothalamic area, zona incerta, and also in the medial geniculate nucleus. In the midbrain and pons, CRF neurons are expressed in the periaqueductal gray, median raphe nucleus, peduncular pontine tegmental nucleus, laterodorsal tegmental nucleus, and in the lateral parabrachial nucleus. In the medulla, CRF neurons are known to exist in the inferior olive and nucleus of the solitary tract [3-6]. CRF neuron has been proposed to play roles in a variety of physiological functions including endocrine stress response [3] , feeding behavior [7], autonomic regulation [8, 9], emotional responses [10], and cerebellar plasticity [11].

The CRF neurons are regulated by numerous neural inputs, including noradrenaline (NA) [12-14], glutamate [15], and γ-aminobutyric acid (GABA) [15]. The noradrenergic afferents make direct synaptic contacts with CRF neurons [16], but they may affect CRF neuronal activity indirectly via glutamatergic or GABAergic interneurons [15, 16]. CRF neurons

present in the PVH, particularly after adrenalectomy, may also express AVP and these neurons are classified as parvocellular (from the Latin, ‘‘parvus’’– meaning small) because of their small size compared with the large size magnocellular neurons and they project to the external zone of the median eminence and release their product to the pituitary portal circulation in response to stress [17-19]. CRF neurons in this area co-express other peptides including AVP, enkephalins, cholecystokine and angiotensin II, and are intermingled with other neuroendocrine neurons such as oxytocin (OXT)-, thyrotropin-releasing hormone (TRH)-, and somatostatin (SRIF), galanin, growth hormone releasing hormone and tyrosine hydroxylase expressing dopaminergic neurons [20]. However, most AVP neurons present in the PVH and in the supraoptic nucleus are magnocellular, and these neurons project to the posterior pituitary through the internal zone of the median eminence [1, 19, 21]. Glucocorticoid (GC), secreted from the adrenals, is the major humoral factor that inhibits the activity of the CRF neurons in the parvocellular PVH and constitutes the negative-feedback loop of the HPA axis [22, 23].

CRF expression is markedly increased in the rat PVH after bilateral adrenalectomy, and this increase can be suppressed by glucocorticoids [1, 24]. The glucocorticoid suppression is specific for the PVH because CRF mRNA expression is unaffected or up-regulated in, for example, the central nucleus of the amygdala or the supraoptic nucleus. The molecular mechanisms for negative glucocorticoid regulation of CRF expression are not fully understood. Glucocorticoid receptors (GRs) are required, but their interactions with specific DNA-regulatory sequences and other transcription factors may be cell-type specific [1].

AVP itself is a weak ACTH secretagogue, but it potentiates the stimulatory effects of CRF on ACTH release from the corticotrophs. AVP in the parvocellular neurons of the PVH are also negatively regulated by glucocorticoids and it is up regulated with withdrawal of the negative feedback by adrenalectomy [25, 26].

Despite considerable efforts in previous studies, it has been hard to unravel the cellular physiological mechanisms for regulating CRF neurons since they cannot be distinguished morphologically from other neuroendocrine neurons, e.g., vasopressin (AVP)-, oxytocin (OXT)-, thyrotropin-releasing hormone (TRH)-, and somatostatin (SRIF)-producing neurons. On the other hand visualizing central sites of endogenous mouse CRF expression through immunohistochemistry has proved difficult without prior brain administration of compounds

such as colchicine [5, 27, 28] that inhibit axonal transport and promote the somatic accumulation of neuropeptides but this approach makes physiological experiments unreliable. The efforts to develop an animal model that enables visualization of CRF neurons without staining have not been successful, even in mice generated by bacterial artificial chromosome (BAC) transgenic strategy [29]. Recently, Wamsteeker Cusulin and colleagues reported a method for visualizing CRF neurons by crossing a *Crh-IRES-Cre* knock-in mouse with a TdTomato reporter *(Ai14)* [28, 30].

Itoi and colleagues generated two mouse lines to visualize CRF neurons by Venus (modified yellow fluorescent protein), and yet, the Venus expression is under the control of the CRF promoter and responds to the changes in *milieu interieur*. In the *CRF-Venus* mouse, the Venus gene was inserted to the CRF gene by homologous recombination so that CRF neurons could be visualized by Venus. A DNA fragment, which carried Venus sequence and pgk-1 promoter-driven neomycin phosphotransferase gene (Neo) flanked by two Flp recognition target (frt) sites, was inserted into the translation initiation site of the exon 2 of CRF gene under the promoter of CRF. With an identical strategy, *CRF-iCre* knock-in mouse was generated by Itoi and colleagues. In the *CRF-iCre*, iCre sequence was inserted at the CRF genomic locus, and otherwise, all the genomic sequences were identical to those of the *CRF-Venus* mouse. Another mouse line, *CRF-VenusΔneo* was also generated; in the *CRF-VenusΔneo*, neomycin phosphotransferase gene (Neo) was deleted from the genomic sequence of the CRF-Venus mouse. By crossing an EGFP-reporter (*CAG-CAT-EGFP*) with the *CRF-iCre*, $Tg^{CAG\text{-}CAT\text{-}EGFP/wt}$;$CRF^{iCre/wt}$ (*EGFP/CRF-iCre*) mouse line was obtained. In a similar manner, $Tg^{CAG\text{-}CAT\text{-}Z/wt}$;$CRF^{iCre/wt}$ (*Z/CRF-iCre*) was obtained by crossing *CRF-iCre* with a lacZ (an E. coli β-galactosidase)-reporter (*CAG-CAT-Z*) mouse. In these reporter mice, either the EGFP or lacZ gene was driven by the CAG promoter. In addition, the chloramphenicol acetyltransferase (CAT) gene, flanked by the loxP sequence, was located between the CAG promoter and the lacZ gene.

The main purpose of the study was immunohistochemical characterization of Venus/EGFP expression in the CRF neuron of different mouse lines. The second purpose of this study was to examine whether the Venus expression in the *CRF-Venus* mouse is dependent on the states of endogenous glucocorticoids (GC), corticosterone (B), by GC deprivation or administration of excess B. Since parvocellular AVP is responsive to GC levels, it was also examined

whether the expression of copeptin, a peptide encoded within AVP gene, is GC-dependent in Venus neurons of *CRF-Venus* mouse.

Therefore, the present research was undertaken with the following specific objectives:

1. Distribution and comparison of Venus expression in the PVH between *CRF-Venus* and *CRF-Venus*Δ*neo* mouse.
2. Distribution of more constitutive EGFP expression in the PVH of *EGFP/CRF-iCre* mouse.
3. Localization of Venus and EGFP-labeled neurons with vasopressin (AVP), oxytocin (OXT), somatostatin (SRIF) and thyrotropin-releasing hormone (TRH) in the *CRF-Venus* and *EGFP/CRF-iCre* brain respectively.
4. Distribution of Venus and EGFP-labeled neurons in the outside of PVH of all mouse line.
5. Glucocorticoid dependent expression pattern of Venus neurons in the PVH of *CRF-Venus* mouse.

Materials and methods

2.1. Generation of *CRF-Venus*, *CRF-VenusΔneo*, *CRF-iCre*, *Z/CRF-iCre, and EGFP/CRF-iCre* mouse.

Mice carrying Venus or iCre in the *Crf* genomic locus were produced by homologous recombination using the C57BL/6N ES cell line RENKA [31]. A targeting vector, constructed in accordance with the mouse genomic DNA databases, contained exon 1 and 2 of *Crf* gene with a 5.8 kb upstream- and a 4.2 kb downstream homologous genomic DNA fragment and the diphtheria toxin gene for negative selection (Figure 1). A DNA fragment, which carried Venus- or iCre sequence and pgk-1 promoter-driven neomycin phosphotransferase gene (Neo) flanked by two Flp recognition target (frt) sites, was inserted into the translation initiation site of the exon 2. Homologous recombination in the ES cells and chimeric mice production were carried out as described previously [31] . Homologous recombinants were identified by Southern blot analyses: Hind III-digested DNA fragments, hybridized with the 5'-probe, were 15.2 kb, 8.7 kb, and 9.1 kb for wild-type (WT)-, targeted Crf-Venus-, and targeted Crf-iCre allele, respectively; Nhe I-digested DNA fragments, hybridized with the 3'-probe, were 8.8 kb, 11.5 kb, and 11.8 kb for WT-, targeted Crf-Venus-, targeted Crf-iCre allele, respectively; Nde I-digested DNA, hybridized with Neo probe, were 11.7 kb and 12.0 kb for targeted Crf-Venus- and targeted Crf-iCre allele, respectively. ES cell clones with the correct recombination were used to yield chimeric mice as described previously [32] . Chimeric mice were mated with C57BL/6N WT mice, and offspring were used for breeding and experiments. For all subsequent breeding, genotypes were determined by PCR analyses of digested mice tail samples. The following primers were used for PCR: forward, 5'-GACCAATCTTACCTTTCTCC-3'; reverse, 5'-AGAAGTCGTGCTGCTTCATG-3' for Crf-Venus allele, and forward, 5'-GACCAATCTTACCTTTCTCC-3'; reverse, 5'-AGGTGGCATCCACAGGGAGG-3' for Crf-iCre allele.

CRF-Venus heterozygous mice and *CRF-iCre* heterozygous mice were generated by breeding with wild-type C57BL/6N mice (CLEA, Tokyo, Japan). Crossing the *CRF-iCre/wt* with either *CAG-CAT-Z/wt* [33] or *CAG-CAT-EGFP/wt* [34] yielded $Tg^{CAG\text{-}CAT\text{-}Z/wt}$;$CRF^{iCre/wt}$ *(Z/CRF-iCre),* or $Tg^{CAG\text{-}CAT\text{-}EGFP/wt}$;$CRF^{iCre/wt}$ (*EGFP/CRF-iCre*) mouse. The iCre-mediated recombination was verified by X-gal staining in the *Z/CRF-iCre* and EGFP staining in the

EGFP/CRF-iCre (*vide infra*).

For the generation of *CRF-VenusΔneo* heterozygous mice (Figure 1), firstly *CRF-Venus* heterozygous mice was crossed with *Actb-Flp* knock-in mice (*Abe et al.,* unpublished) .In the obtained *CRF-venus;Actb-Flp,* Neo cassette was removed and they were used to generate *CRF-VenusΔneo* without Actb-Flp by crossing with wild type C57BL/6N mice.

2.2. Animal housing and Colchicine infusion

Mice were housed at constant temperature (23°C) and humidity (55%) with 12h/12h light-dark cycle (lights on from 07:00-19:00) and allowed free access to drinking water and pellets. Male *CRF-Venus* mice were used for glucocorticoid dependent Venus expression study but sex did not consider for other distribution study. Mice were anesthetized deeply with chloral hydrate (400 mg/kg), and intracerebroventricularly (i.c.v) treated with colchicine (30 μg dissolved in 2 μl saline) by unilateral injection through a glass capillary placed into the lateral ventricle under stereotaxic control (coordinates from Bregma: anteroposterior, −0.2 mm; lateral, −0.9 mm; dorsoventral from dura, −2.0 mm).

2.3. Surgery and stress less removal of corticosterone

A group of *CRF-Venus* mice underwent bilateral adrenalectomy or sham-operation. Bilateral adrenalectomy (ADX) was performed via the dorsal route under chloral hydrate (400 mg/kg body weight) anesthesia. The surgical procedure of sham-operation was identical to that of ADX except that both adrenals were exposed but not removed. *Dallman and Jacobson et al*. model was employed for stress less removal of corticosterone (B) [35, 36] . For sham group, mice were given only drinking fluid (0.45% saline and 2.5% dextrose). On the other hand, all adrenalectomized mice were given B (25 μg/ml) in drinking fluid for 5 days and then, mice were separated into two groups: one group was deprived of B for 7 days [B (−)] while the other received B administration continuously (B surplus). Mice drank a significantly greater volume of fluid following ADX and the amount of corticosterone that was taken daily by mouse belongs to B surplus group was estimated to be 295 ± 20 μg (Table 1). Twelve days after surgery, colchicine was injected intracerebroventricularly (i.c.v), mice were perfused 20 hours later, and then brains were extracted for immunohistochemistry.

2.4. Brain perfusion and sectioning

Mice were deeply anesthetized with chloral hydrate (i.p.) and were perfused transcardially through the ascending aorta with approximately 10 ml of 0.9% saline, followed by 10 ml of 4% paraformaldehyde (PFA) containing 0.1 M phosphate buffer (PB), pH 7.4. After perfusion, brains were taken out immediately and immersed overnight in 4% paraformaldehyde at 4°C, followed by replacement with 30% sucrose containing 0.1 M PB until the tissue sank. The fixed brains were then embedded in Tissue Tek ™ (Sakura Fine Technical Co. Ltd., Tokyo, Japan) at −40°C and stored at −80°C until use. Thirty μm coronal sections were cut by a cryostat (Microm HM505N, Heidelberg, Germany). The sections were kept in a cryoprotectant (30% ethylene glycol + 15% sucrose) solution and stored at 4°C until immunohistochemistry.

2.5. Immunohistochemistry and X-gal staining

2.5.1 Single Immunohistochemistry: Venus or EGFP

For immunohistochemistry of Venus of *CRF-Venus* and *CRF-VenusΔneo* mouse or EGFP of *CRF-EGFP* mouse, free-floating sections were washed with phosphate-buffered saline (PBS). Then the sections were incubated for 18 h at 4°C with primary antibody rat anti-GFP (1:10,000; Nacalai Tesque, Kyoto, Japan) and 5% donkey serum as blocking solution. Then the sections were washed with PBS and incubated with secondary antibody anti-rat IgG conjugated with Alexa488 (donkey, 1:250; Invitrogen, Eugene, OR) for 2 h at room temperature. After washing with PBS, the sections were mounted on poly-L-lysine-coated glass slides using glycerin and observed both under fluorescent microscope (Leica DMR, Wetzler, Germany) and confocal microscope (Leica DM2500, Mannheim, Germany).

2.5.2 Double Immunohistochemistry: Venus or EGFP with CRF, Copeptin, Vasopressin (AVP), Oxytocin (OXT), SRIF, TRH.

The free floating sections were washed with phosphate-buffered saline (PBS) and incubated with 5% donkey serum as blocking solution and one or a combination of the following

primary antibodies: rat anti-GFP (1:10,000; Nacalai Tesque, Kyoto, Japan), rabbit anti-CRF (1:50,000; Shibasaki [37]), and goat anti-copeptin (1:15,000; Santa Cruz, Dallas, TX), rabbit anti-AVP (1: 5,000; [38]), rabbit anti-OXT (1:10,000; Chemicon, Billerica, MA), goat anti-SRIF (1:500; Enzo Life Science, Farmingdale, NY), and sheep anti-TRH (1:100; [39]). The anti-GFP antibody was used to identify EGFP- and Venus-expression [40].The incubation period was 18 hours except for TRH (72 hours) 4°C. Then the sections were washed again with PBS and incubated with secondary antibodies for 2 hours at room temperature. Anti-rat IgG conjugated with Alexa488 (donkey, 1:250; Invitrogen, Eugene, OR) was used as the secondary antibody for EGFP or Venus, anti-rabbit IgG conjugated with Alexa647 (donkey, 1:500) for CRF, and anti-goat IgG conjugated with Alexa647 (donkey, 1:500) for copeptin, anti-rabbit IgG conjugated with Alexa647 (donkey, 1:500) for AVP and OXT, anti-goat IgG conjugated with Alexa647 (donkey, 1:500) for SRIF, and anti-sheep IgG conjugated with Alexa555 (donkey, 1:500) for TRH. The stained sections were captured by a confocal microscope (Leica DM2500, Mannheim, Germany).

2.5.3 Double Immunohistochemistry: Venus or EGFP with CRF in the medial preoptic area, bed nucleus of stria terminalis, sensory motor cortex, central nucleus of amygdala, Barrington's nucleus and inferior olivary nucleus.

Colchicine was infused differently from aforementioned procedure. Small amount (4 μg dissolved in 0.4 μl saline) of colchicine was infused by bilateral injection under same stereotaxic control (coordinates from Bregma: anteroposterior, −0.2 mm; lateral, ±0.9 mm; dorsoventral from dura, −2.0 mm). Mice were perfused 72 h later, and then brains were collected. The immunohistochemistry procedure was same that described in earlier section except using of anti-rat IgG conjugated with Alexa 594(1:500) instead of Alexa 647 as secondary antibody.

2.5.4 X-gal staining:

For histological detection of β-galactosidase, *Z/CRF-iCre* mice were fixed transcardially with 4% paraformaldehyde in PBS. Coronal brain sections of 100 μm were cut by a vibratome (VT1000, Leica, Germany, Wetzlar). The brain sections were incubated at 37°C for 4 hours in PBS containing 5 mM potassium hexacyanoferrate (III), 5 mM potassium hexacyanoferrate (II), 2 mM $MgCl_2$, and 1 mg/ml 5-bromo-4-chloro-3-indolyl-β-D-galactopyranoside (X-gal). Stained sections were observed under a microscope (MZ 16 FA, Leica) and captured by a digital camera (Pixera, Penguin 600CL-CU, Santa Clara, CA).

2.6 Cell counting and densitometry

Serial sections were taken from the entire rostrocaudal extent of the PVH, and five consecutive sections that contained the highest number of CRF and Venus neurons were used for counting and densitometry. Following immunohistochemical staining, cell images were captured by a confocal scanning microscope (Leica DM2500, Mannheim, Germany). Cell number was counted manually by using the Cell Counting Plug-in of Image J software (http://rsbweb.nih.gov/ij/). Densitometry was performed by Image J Basic Intensity Quantification Procedure; the background density was subtracted from the signals using a thresholding macro (BG_subtraction_from_ROI). The mean of the integrated density values (mean density × area), calculated for the 5 sections, was used for statistical analysis.

2.7 Statistical analysis

Graph pad prism 5 software was used for statistical analysis, one way ANOVA followed by Tukey's *post-hoc* test was carried out for comparison among three groups and paired t-test for comparison between two groups. Data are expressed as the means ± SEM. $P < 0.05$ was considered to be significant statistically.

Results

3.1. Distribution and comparison of Venus expression in the PVH between *CRF-Venus* and *CRF-Venus*Δ*neo* mouse: Venus with CRF expression was examined in the PVH of colchicine treated naive mouse by double immunohistochemistry (Figure 2). In *CRF-Venus* mouse there was a considerable discrepancy between Venus and CRF expression whereas the number of Venus and CRF neurons were similar in the PVH of *CRF-Venus*Δ*neo* mouse. In *CRF-Venus* mouse, some Venus cell was of lower intensity and some was of higher intensity. But in *CRF-Venus*Δ*neo* mouse, all Venus cell was expressed with similar intensity. The number of Venus neurons in the PVH of *CRF-Venus*Δ*neo* mouse was significantly greater than that of *CRF-Venus* mouse (Figure 2 and 3; Table 2). In the *CRF-Venus* mouse, a majority (57 ± 1%) of Venus neurons expressed CRF but approximately one third (38 ± 2%) CRF neurons expressed Venus. On the other hand, most of the Venus neurons (84 ± 5%) co-express CRF and vice versa (84 ± 4%) in the *CRF-Venus*Δ*neo* mouse (Figure 2 and 4; Table 2).

3.2. Distribution of more constitutive EGFP expression in the PVH of *EGFP/CRF-iCre* mouse: Co-localization of EGFP with CRF was also examined in the PVH of colchicine treated naive *EGFP/CRF-iCre* mouse by double immunohistochemistry. In this mouse line, EGFP was expressed constitutively and in contrast to the *CRF-Venus* mouse, the number of EGFP was greater and similar to the number of CRF (Figure 5). On the other hand, most (85 ± 2%) of the EGFP neurons were co-expressed with CRF, and vice versa (81 ± 4%) in the PVH of this mouse line (Figure 6).

3.3. Localization of Venus and EGFP-labeled neurons with vasopressin (AVP), oxytocin (OXT), somatostatin (SRIF) and thyrotropin-releasing hormone (TRH) in the PVH of *CRF-Venus* and *EGFP/CRF-iCre* mouse brain respectively: Double immunohistochemistry was carried out to examine whether Venus -expressing neurons co-express with vasopressin (AVP), oxytocin (OXT), somatostatin (SRIF), or thyrotropin-releasing hormone (TRH) in the PVH of naive colchicine-treated *CRF-Venus* mice. The Venus neurons did not express OXT, SRIF, or TRH. They were also devoid of AVP expression, with very few exceptions (Figure 7). The same experiment was carried out for *EGFP/CRF-iCre* mouse with identical procedure and EGFP neurons were also devoid of AVP

expression, with very few exceptions and did not express OXT, SRIF, or TRH (Figure 8).

3.4. Distribution of Venus-labeled neurons in the outside of PVH of *CRF-Venus* mouse brain: In colchicine-treated naive *CRF-Venus* mouse, distribution of Venus neurons was examined by single immunohistochemistry. Modest numbers of Venus neurons were observed in the medial preoptic area (Figure 9A; Table 3). The greatest density of stained cell was found just ventral to the anterior commissure and periventricular parts of the area. Both dorsal and ventral portions of the bed nucleus of the stria terminalis (BNST) had a moderate content of Venus cells throughout its rostrocaudal extent but the highest density was visualized at the lateral part of the area (Figure 9B; Table 3). A considerable number of Venus cells were also found in the piriform cortex (Figure 9C; Table 3) and scattered cells evenly distributed throughout the cerebral cortex (Figure 9D; Table 3). The vast majorities of cortical cells were distributed within layers II and III, bipolar in size and were oriented perpendicular to the surface of the cortex. Besides the central amygdaloid nucleus (CeA), which contained numerous Venus cells (Figure 9E; Table 3), Venus cells were also seen both in the medial and lateral amygdaloid nucleus. A modest content of Venus cells were also expressed in the laterodorsal tegmental nucleus (Figure 9F; Table 3) and Barrington's nucleus (Figure 9G; Table 3). In inferior olivary nucleus (Figure 9H; Table 3), a rich content of fibers and cells were found. Modest number of Venus-expressing neurons and fibres were also present in olfactory tubercle (Figure 10A; Table 3), and small number in the median raphe nucleus (Figure 10G; Table 3), lateral parabrachial nucleus (Figure 10I; Table 3) .Scattered cells were also found in lateral septum, accumbens nucleus, lateral hypothalamic area, periaqueductal gray, peduncular pontine tegmental nucleus, and nucleus of the solitary tract (Figure 10B, C, D, F, H and J respectively ; Table 3). Venus-expressing nerve endings were also confined in the external layer and very scantly distributed in the internal layer of the median eminence (Figure 10E).

3.5. Distribution of Venus-labeled neurons in the outside of PVH of *CRF-Venus*Δ*neo* mouse brain: In colchicine-treated naive *CRF-Venus*Δ*neo* mouse, distribution of Venus neurons was examined by single immunohistochemistry. Venus neurons were distributed in all brain regions that described for CRF-Venus mouse (Figure 11and 12; Table 3) and the expression pattern was also similar except median eminence. Venus-expressing nerve endings were restricted in the external layer of median eminence but the density was greater than that

of *CRF-Venus* mouse.

3.6. Distribution of β–galactosidase-labeled neurons in the *Z/CRF-iCre* mouse brain: In naive *Z/CRF-iCre* mouse β-galactosidase neurons examined by X-gal staining and the distribution pattern was also similar to Venus expression of *CRF-Venus* mouse (Figure 13).

3.7. Distribution of EGFP-labeled neurons in the outside of PVH of *EGFP/CRF-iCre* mouse brain: In colchicine-treated naive *EGFP/CRF-iCre* mouse brain, distribution of EGFP was examined by identical procedure. EGFP neurons were observed in brain regions including the medial preoptic area, dorsal and ventral portions of the bed nucleus of the stria terminalis, cerebral cortex, central nucleus of the amygdala, piriform cortex, laterodorsal tegmental nucleus, Barrington's nucleus, inferior olivary nucleus (Figure 14 ; Table 3). EGFP-expressing neurons were also present in olfactory tubercle, lateral septum, accumbens nucleus, lateral hypothalamic area, periaqueductal gray, median raphe nucleus, peduncular pontine tegmental nucleus, lateral parabrachial nucleus, and nucleus of the solitary tract (Figure 15; Table 3). EGFP neurons were expressed more constitutively than Venus neurons in *CRF-Venus* mouse brain and the major discrepancy was observed in olfactory tubercle, accumbens nucleus and in piriform cortex where number of EGFP cell was greater than number of Venus neuron of *CRF-Venus* mouse (Table 3). EGFP-expressing nerve endings were also concentrated in the external layer of the median eminence but more prominent than Venus nerve ending of *CRF-Venus* mouse (Figure 15E).

3.8. Co-localization of Venus-labeled neurons with CRF in the medial preoptic area, bed nucleus of stria terminalis (BNST), sensory motor cortex, central nucleus of amygdala, Barrington's nucleus and inferior olivary nucleus of *CRF-Venus* mouse brain: Double immunohistochemistry was carried out to examine the co-localization in the colchicine treated naive mouse. Venus neurons were clearly stained in all area but only dense fibers and small number of CRF neurons were visualized in most of the area. In the medial preoptic area, a considerable number of CRF neurons were found although the number was smaller than Venus neurons but most of them (approximately 80%) were expressed Venus (Figure 16, A row). A rich content of CRF fibers and small number of CRF neurons were

visualized in the BNST and most of them (approximately 75%) expressed Venus (Figure 16, B row). In Sensory motor cortex, both CRF and Venus cells were clearly stained and most of the Venus cells expressed CRF although some cells were either Venus or CRF (Figure 16, C row). Central nucleus of amygdala had a dense content of CRF fiber and very few well-structured CRF neuron and most of them were colocalized with Venus (Figure 17, A row). In Barington's nucleus, both types of cells were clearly stained and majority of Venus cell (approximately 70%) expressed CRF and vice versa (Figure 17, B row). The distributed area of densely CRF fibers was exactly same of the area of well stained Venus neurons in inferior olivary nucleus. Some CRF neurons also recognized and they were colocalized with CRF neurons (Figure 17, C row).

3.9. Co-localization of EGFP-labeled neurons with CRF in the medial preoptic area, bed nucleus of stria terminalis (BNST), sensory motor cortex, central nucleus of amygdala, Barrington's nucleus and inferior olivary nucleus of *EGFP/CRF-iCre* mouse brain: Double immunohistochemistry was carried out to examine the co-localization with identical manner that used for *CRF-Venus* mouse and the colocalization pattern was almost similar except Barrington's nucleus (Figure 18 and 19). In Barrington's nucleus the number of EGFP was greater than CRF number and prominently expressed than Venus neurons of CRF-Venus mouse. In this mouse line, more than 90% CRF colocalized with EGFP in contrast approximately 70% EGFP neuron was colocalized with CRF.

3.10. Distribution and glucocorticoid dependent expression of Venus neurons in the PVH of *CRF-Venus* mouse: Distribution and glucocorticoid dependent Venus expression with CRF neuron was examined in the PVH of *CRF-Venus* mouse by double immunohistochemistry (Figure 2). In sham operated or control *CRF-Venus* mouse there was a considerable discrepancy between Venus and CRF expression (Figure 20, control; Table 4). The number of CRF neurons increased significantly after B deprivation, but there was no significant increase in the number of Venus neurons [Figure 20 and 21, B (−); Table 4]. In mice which were given a high dose of B continuously, the numbers of Venus- and CRF neurons decreased markedly (Figure 20 and 21, B surplus; Table 4). In addition, immunofluorescent intensity of Venus and CRF, as was quantified by densitometry, increased after B deprivation by 54 ± 16% (Figure 22) and 94 ± 31% (Figure 23), respectively. The immunofluorescent intensity of Venus and that of CRF also decreased by 54 ± 7% (Figure 22) and 93 ± 3% (Figure 23) respectively after giving excess amount of B continuously.

In the control (sham-operated) mouse, a majority (approximately 60%) of Venus neurons expressed CRF. On the other hand, only one third (approximately 33%) of CRF neurons expressed Venus (Figure 20 and 24, control; Table 4); thus, there was a considerable discordance between Venus- and CRF expression. For the purpose of activating CRF promoter, a group of mice was deprived of B for one week. Most of the Venus cells (approximately 80%) became expressing of CRF following B deprivation [Figure 20 and 24, B (−); Table 4]. In mice which were given a high dose of B continuously, the colocalization of Venus- and CRF neurons decreased markedly [(approximately 20%) Figure 20 and 24, B surplus; Table 4].

3.11. Expression of copeptin in the Venus cells following B deprivation in the PVH of *CRF-Venus* mouse: Distributions of Venus- and copeptin-expressing neurons were examined by double immunohistochemistry in the PVH of the *CRF-Venus* mouse (Figure 25). There was no significant change in the number of Venus neurons after B deprivation but markedly decreased in the mice which were given high dose of B continuously. In sham operated and B surplus group animals, the number of copeptin was similar but the number increased significantly after B deprivation (Figure 25 and 26; Table 5). Very few Venus cells co-expressed copeptin in sham-operated animals (Figure 25 and 27, control; Table 5). One week following B deprivation, however, approximately half of the Venus cells expressed copeptin [Figure 25 and 27, B (−); Table 5]. In animals which were given a high dose of B, only a very few Venus cells expressed copeptin (Figure 25 and 27, B surplus; Table 5). By close observation of the copeptin expression, a majority of the Venus/copeptin dual expressing neurons was of lower intensity [arrows, Figure 25, B (−), insets]. In contrast, high-intensity copeptin neurons predominated among those without Venus expression (arrowheads) although low-intensity ones were also present (asterisk).

Discussion

4.1. Comparative distribution of Venus expression in the PVH of *CRF-Venus* and *CRF-VenusΔneo* mouse brain.

In the PVH of *CRF-Venus* mouse the number of Venus neurons was much smaller than CRF neuron and the intensity of Venus cell was variable that means some cell was of lower intensity and some cell was of higher intensity. A majority of Venus-expressing neurons expressed CRF in the physiological GC state, but a considerable number of neurons expressed only Venus or CRF. In this mouse line PGK–Neo cassette (a hybrid consisting of the phosphoglycerate kinase I promoter driving the neomycin phosphotransferase gene which was flanked by Flp recognition target (frt) sites) was inserted as a positive selection marker for homologous recombination in embryonic stem cells. On the other hand, in *CRF-VenusΔneo* mouse (PGK–Neo was deleted by breeding *CRF-Venus* mouse with Actb-Flp knock-in mouse) Venus cell was expressed with similar intensity and the number was similar to the number of CRF neuron in the PVH, and most of the Venus neurons expressed CRF and vice versa. It has been reported that marker genes (PGK-Neo) can interfere the transcription and splicing of the target and neighboring gene, thereby introducing ambiguities in genotype –phenotype relationship but the mechanism is not yet clearly understood [41-43]. A final and very clear example of the effects of the *PGKneo* cassette is provided by the work of Fiering et al. (1995) who designed a targeted deletion of the 5′ DNase hypersensitive site 2 (5′ HS2) of the locus control region (LCR) of the β-globin locus. They showed that the insertion of PGK–Neo abrogates the expression of multiple globin genes downstream from the cassette. Deletion of the selectable marker cassette results in restoration of LCR activity [44] . Pham et al. (1996) also reported that insertion of PGK–Neo into the murine granzyme B gene abrogates the expression of several granzyme genes within the granzyme B gene cluster [42]. N.Tamamaki et al. (2003) also evaluated the expression of GFP in *GAD67-GFP* mice and *GAD67-GFPΔneo* mice and they showed that in latter mice GFP intensity was much denser than that of earlier one [45]. However, the exact reason in this regard is not clear at this moment and further detail study is required to elucidate it.

4.2. Distribution of β–galactosidase-labeled neurons in the *Z/CRF-iCre* brain and more constitutive EGFP expression in the PVH of *EGFP/CRF-iCre* mouse brain.

The brain distribution of β-galactosidase-expressing cells in the *Z/CRF-iCre* mouse brain and EGFP-expressing cells in the PVH of *EGFP/CRF-iCre* was similar to that of CRF neurons reported in previous literature [4, 27, 29, 46], indicating that the iCre-mediated recombination took place in a CRF-promoter dependent manner. It is noticeable that most EGFP neurons expressed CRF in the PVH of *EGFP/CRF-iCre*. The more constitutive EGFP expression, compared to the Venus expression, could be explained by the constitutive activity of CAG promoter, flanking the CAT-EGFP sequence of the reporter mouse [34]. Recently, Wamsteeker Cusulin and colleagues reported a mouse, in which TdTomato is driven by CAG promoter, for visualizing CRF neurons [28]. Both their driver mouse (*Crh-IRES-Cre*) and ours (*CRF-iCre*) are generated by the knock-in strategy, so the chromosomal locus, where the targeting DNA constructs were inserted, is identical, but the cell specific gene expression may also be dependent on the sequences of targeting vectors as well as the properties of reporters. Therefore, a precise comparison would be desirable as regards the distribution of TdTomato- and EGFP-expressing neurons, within as well as outside the PVH.

4.3. Localization of Venus and EGFP-labeled neurons with vasopressin (AVP), oxytocin (OXT), somatostatin (SRIF) and thyrotropin-releasing hormone (TRH) in the PVH of *CRF-Venus* and *EGFP/CRF-iCre* mouse brain respectively.

The Venus or EGFP cells were devoid of SRIF, TRH and almost devoid of AVP confirming the selectivity of Venus or EGFP expression in CRF neurons. The Venus/EGFP-expressing neurons did not express OXT, either. A small population of OXT neurons was reported to co-localize with CRF in the rat, but it may not be in conflict with the present results; the OXT/CRF co-expressing neurons are most likely magnocellular neurons [47] , whereas Venus or EGFP cells may be mostly parvocellular neurons, judging from the electrophysiological hallmarks.

4.4. Distribution of Venus/EGFP neuron in the outside of PVH of *CRF-Venus*, *CRF-Venus*Δ*neo*, and *EGFP/CRF-iCre* mouse brain.

CRF-Venus and *CRF-Venus* Δ*neo* mouse was generated to visualize CRF neurons with Venus fluorescence. In both mouse lines, the Venus-expressing cells were present in brain regions including olfactory tubercle, lateral septum, accumbens nucleus, medial preoptic area, dorsal and ventral portions of the bed nucleus of the stria terminalis, cerebral cortex, central nucleus of the amygdala, piriform cortex, lateral hypothalamic area, periaqueductal gray, median raphe nucleus, peduncular pontine tegmental nucleus, laterodorsal tegmental nucleus, Barrington's nucleus, lateral parabrachial nucleus, nucleus of the solitary tract, and inferior olivary nucleus that was highly consistent with the distribution of CRF neurons, reported previously in mice [29, 46] and rats [4, 5, 27]. In the *EGFP/CRF-iCre* mouse EGFP expressed more constitutively in most of the aforementioned area could be explained by its expression under a strong promoter. But the most contrasting area was olfactory tubercle, accumbens nucleus, piriform cortex, central nucleus of amygdala and inferior olivary nucleus where EGFP number was greater than Venus number of *CRF-Venus* mouse and also inconsistent with CRF number according to previous studies [4, 29]. The reason is not clear at this moment whether it was because of ectopic expression or different expression pattern between at embryonic stage or adult stage of mouse. To elucidate it further detail study is required on expression and distribution pattern of mouse CRF and Venus/EGFP in those areas both at embryonic and adult stage in all mouse lines. It had been reported that in the median eminence CRF- immunoreactive nerve fibers are localized in large numbers in the median to paramedian portions of the external layer, extending perpendicularly from the internal layer to the capillary loops of the portal vessels. A small number of fine CRF-immunoreactive nerve fibers run tangentially in the internal layer [18, 19, 48]. Venus/EGFP nerve endings were also localized similarly in the median eminence.

4.5. Co-localization of Venus and EGFP-labeled neurons with CRF in the medial preoptic area, bed nucleus of stria terminalis (BNST), sensory motor cortex, central nucleus of amygdala, Barrington's nucleus and inferior olivary nucleus in the colchicine treated naive *CRF-Venus* and *EGFP/CRF-iCre* mouse brain.

Double immunohistochemistry was carried out to examine the co-localization of Venus/EGFP with CRF in the mentioning area but only Venus/EGFP neurons were clearly stained in all

area. In contrast, only dense fibers and small number of CRF neurons was visualized in most of the area even after small dose and long lasting administration of colchicine. However, these results also demonstrated the necessity to develop studied mouse lines to study CRF neuron in these areas. Double in situ hybridization or dual in situ and immunohistochemistry are required to explore the colocalization in the mentioning area.

4.6. Glucocorticoid dependent Venus expression in the PVH of *CRF-Venus* mouse.

The co-localization of Venus with CRF was examined more precisely in the PVH of the *CRF-Venus* mouse. At physiological GC state, a majority of Venus-expressing neurons expressed CRF. However, a considerable number of neurons expressed only Venus or CRF because CRF promoter activity may be partly suppressed by B under the physiological condition [49] .So we examined the effect of B deprivation to see if it may enhance co-localization of Venus with CRF.

One week following B deprivation, the number of Venus cells co-expressing CRF increased significantly, and most Venus neurons became expressing of CRF. This raises the possibility that the Venus-expressing cells, in which CRF expression could not be verified in the physiological GC state, may actually be the 'CRF neurons'. In contrast, a majority of CRF neurons did not co-express Venus even after B deprivation, and the reason is not clear at this moment. On the other hand, the immunofluorescent intensity of Venus and CRF increased significantly following B deprivation and was suppressed by excess B administration. Thus, Venus neurons partially recapitulated the GC-dependent responses of PVH-CRF neurons [1, 24, 50].

4.7. Expression of copeptin in the Venus cells following B deprivation in the PVH of *CRF-Venus* mouse.

In a physiological GC state, Venus neurons were almost devoid of copeptin. In contrast, a major proportion of Venus cells expressed copeptin after B deprivation, which was reversed by B administration. It is well known that CRF neurons are capable of producing AVP in the PVH, and both CRF and AVP are regarded secretagogues for adrenocorticotropin in the pituitary [1]. In rats, CRF colocalization with AVP in parvocellular neuroendocrine cells (PNCs) has only been reported when glucocorticoids are removed [51]or after repeated stress

[52]. However, AVP gene expression in CRF neurons is mostly suppressed in the physiological GC state and becomes eminent by GC deprivation [24, 53, 54]. In our study, approximately fifty percent Venus neuron express AVP after glucocorticoid deprivation. Therefore, Venus neurons recapitulated the GC-dependent AVP gene expression in CRF neurons.

However, the genomic construct of *CRF-Venus* mouse was designed so that Venus expression was driven by the CRF promoter. The study demonstrated that Venus usually expressed where CRF neurons known to express and its expression in the PVH was strictly depends on the glucocorticoid state of the animal. This may be an advantage for monitoring dynamic changes in CRF neurons and CRF networks in different glucocorticoid states, including elevated glucocorticoid conditions (e.g., Cushing syndrome) and glucocorticoid deficiency (e.g., Addison's disease). In *CRF- VenusΔneo* mouse, Venus was also inserted under CRF promoter and it was expressed more consistently and pattern of expression was similar to CRF in the PVH but Glucocorticoid dependent Venus expression in this mouse line not yet to be studied. On the other hand, *EGFP/CRF-iCre* and the mouse reported by Wamsteeker Cusulin and colleagues may have the advantage of the ability to more consistently label CRF neurons because EGFP and TdTomato both were inserted under strong promoter and expressed consistently. So the characterizations of the reporter mouse lines confirm faithful recapitulation of central CRF expression and preserved functionality in the regions assessed. So it has been suggested that the integrity and tractability of these mouse lines will prove to be of significant value to CRF-related research.

Tables

Table 1: Calculation of amount of drinking water taken by different group of *CRF-Venus* mouse daily.

	Volume of water taken/day	Amount of B (μg) taken/day
Control	7.3 ± 0.8	-----
B (−)	11.79 ± 0.77 **	----------
B surplus	11.82 ± 0.79 **	295.5 ± 19.75

Amount of drinking water was calculated daily throughout the study. n = 5 for control, n = 4 for B (−) and B surplus; **, P < 0.01 vs. control; Paired t-test.

Table 2: Comparison of number of Venus-, CRF-, or Venus/CRF-expressing neurons in the PVH between *CRF-Venus* and *CRF-VenusΔneo* mouse.

	No. of Venus neurons	No. of CRF neurons	% of Venus neurons expressing CRF	% of CRF neurons expressing Venus
CRF-Venus	49 ± 4	81 ± 3	57 ± 1	38 ± 2
CRF-Venus Δneo	92 ± 4 **	89 ± 4	84 ± 5 *	84 ± 4 **

The mean number of Venus-, CRF neurons in unilateral PVH was calculated using 2 medial sections per animal (n = 3). The mean percentage of Venus-expressing neurons which co-express CRF and that of CRF-expressing neurons which co-express Venus were also calculated. *, $P < 0.05$, **, $P < 0.01$ vs. *CRF-Venus*; Paired t-test.

Table 3: Comparative distribution of Venus and EGFP cell number in the outside of PVH of studied mouse lines.

Brain Region	*CRF-Venus*	*CRF-VenusΔneo*	*EGFP/CRF-iCre*
Olfactory tubercle	**	**	****
Lateral septum	*	*	*
Accumbens nucleus	*	*	****
Medial preoptic area	***	***	****
Bed nucleus of stria terminalis	**	**	***
Cortex	*	*	*
Piriform cortex	***	***	****
Central nucleus of amygdala	***	***	****
Lateral hypothalamus	*	*	*
Periaqueductal gray	*	*	**
Median Raphe nucleus	*	*	*
Peduncular pontine tegmental nucleus	*	**	**
Later dorsal tegmental nucleus	***	***	***
Lateral parabrachial nucleus	*	*	*
Barrington's nucleus	**	**	**
Inferior olive	****	****	****
Nucleus of the solitary tract	*	*	*

*, Scattered cell or Mild number (1-20 cells/section); **, Modest number (21-50 cells/section); ***, Moderate number (51-100 cells/section); ****, High number (>100 cells/section).

Table 4: The number of Venus-, CRF-, or Venus/CRF-expressing neurons in the PVH of *CRF-Venus* mouse

	No. of Venus neurons	No. of CRF neurons	No. of Venus/CRF neurons	% of Venus neurons expressing CRF	% of CRF neurons expressing Venus
control	50 ± 1	93 ± 4	29 ± 2	59 ± 5	32 ± 1
B (−)	52 ± 2	110 ± 3*	41 ± 3*	80 ± 1*	37 ± 1*
B surplus	22 ± 1**,††	27 ± 5**,††	4 ± 1**,††	20 ± 4**,††	18 ± 1**,††

The mean number of Venus-, CRF-, or Venus/CRF-expressing neurons in unilateral PVH was calculated using 5 sections per animal (n = 4). The mean percentage of Venus-expressing neurons which co-express CRF and that of CRF-expressing neurons which co-express Venus were also calculated.

*, $P < 0.05$, **, $P < 0.01$ vs. control; †, $P < 0.05$, ††, $P < 0.01$ vs. B (−); ANOVA followed by Tukey's *post- hoc* test.

Table 5: The number of Venus-, copeptin-, or Venus/copeptin-expressing neurons in the PVH of *CRF-Venus* mouse.

	No. of Venus neurons	No. of copeptin neurons	No. of Venus/copeptin neurons	% of Venus neurons expressing copeptin	% of copeptin neurons expressing Venus
Control	49 ± 7	83 ± 3	1 ± 1	1 ± 1	1 ± 1
B (−)	57 ± 10	143 ± 19*	27 ± 7**	46 ± 8**	18 ± 3**
B surplus	29 ± 3†	85 ± 8†	2 ± 2††	6 ± 3††	2 ± 1††

The mean number of Venus-, Copeptin-, or Venus/copeptin-expressing neurons in unilateral PVH was calculated using 5 sections per animal (n = 4). The mean percentage of Venus-expressing neurons which co-express copeptin and that of copeptin-expressing neurons which co-express Venus were also calculated.
*, $P < 0.05$, **, $P < 0.01$ vs. control; †, $P < 0.05$, ††, $P < 0.01$ vs. B (−); ANOVA followed by Tukey's *post- hoc* test.

Figures

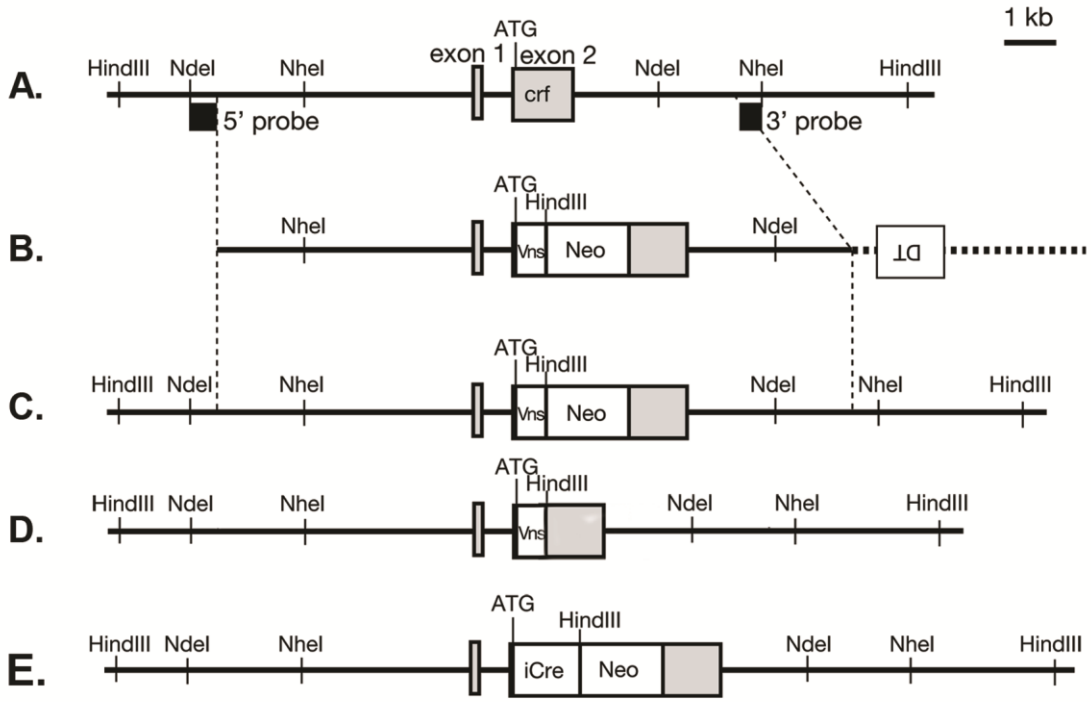

Figure 1: A strategy for knocking Venus (Vns) - or iCre gene into the mouse *crf* genomic locus is presented schematically. A, B, C, D, and E represent the mouse *crf* genome, the targeting vector, the Venus-targeted allele, Venus-targeted allele without neo and the iCre-targeted allele, respectively. By homologous recombination in the ES cells, the Venus (C) or iCre (E), together with the pgk-neomycin resistant cassette (Neo), was inserted at the translation initiation site of the *crf* gene. The exons of the *crf* gene are represented by gray-colored boxes, while Venus and iCre sequences, frt-flanked Neo, and diphtheria toxin (DT) cassette by open boxes. Closed boxes indicate 5'- and 3'-probe regions used for Southern blot analysis.

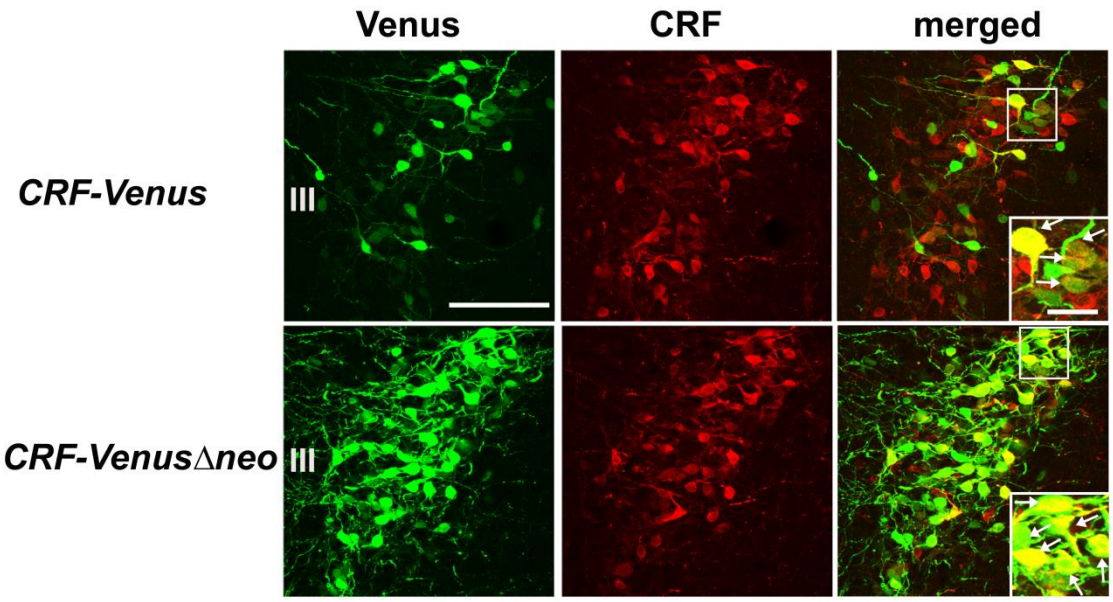

Figure 2: Photomicrographs representing distribution of Venus-expressing neurons (green) and CRF-expressing neurons (red) in the PVH of *CRF-Venus* and *CRF-VenusΔneo* mouse. Insets: circumscribed areas are shown in a higher magnification at the right lower angle of each photomicrograph. Arrows indicate the neurons which express both Venus and CRF. III, third ventricle. Scale bars = 100 μm (25 μm for insets).

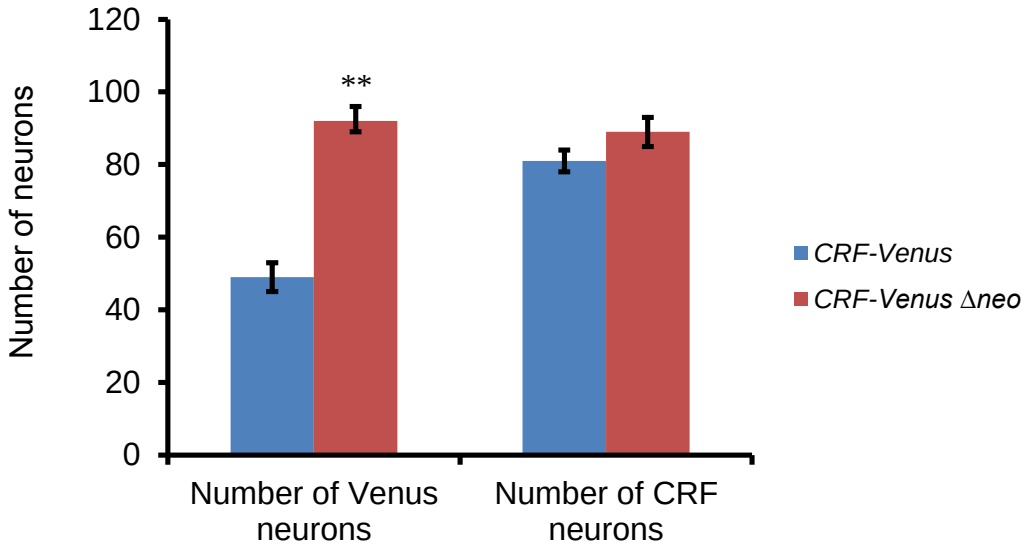

Figure 3: Comparison the number of Venus and CRF neurons per unilateral PVH between *CRF-Venus* and *CRF-VenusΔneo mouse*. Values are mean ± SEM. **, P < 0.01; Paired t-test. n = 3 per group.

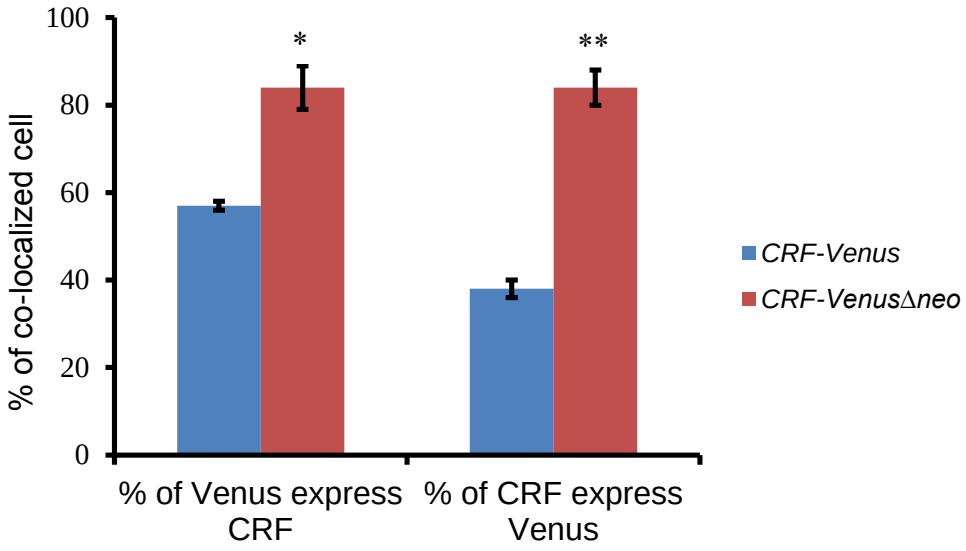

Figure 4: Percentage of Venus cell that express CRF and vice versa in the PVH of *CRF-Venus* and *CRF-VenusΔneo* mouse. Values are mean ± SEM. *, P < 0.05, **, P < 0.01; Paired t-test. n = 3 per group.

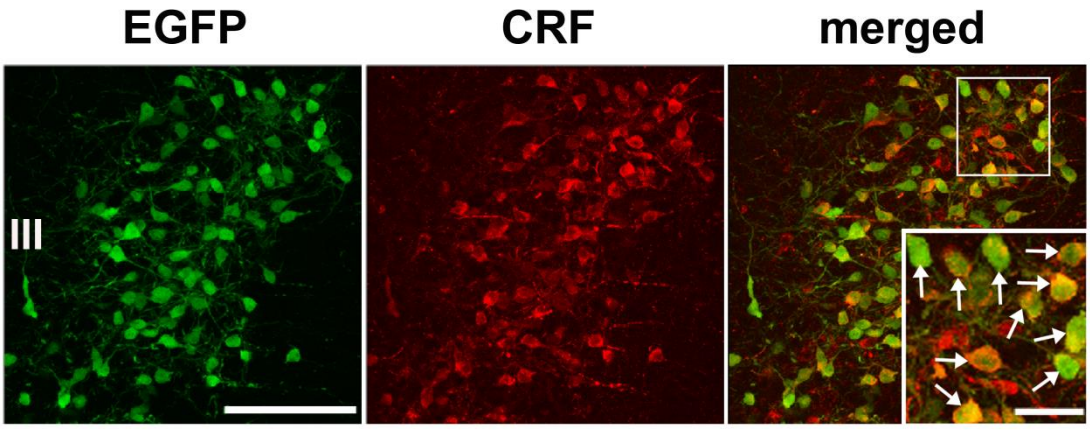

Figure 5: Photomicrographs representing distribution of EGFP-expressing neurons (green) and CRF-expressing neurons (red) in the PVH of *EGFP/CRF-iCre* naive colchicine treated mouse. Inset: circumscribed area is shown in a higher magnification at the right lower angle of photomicrograph. Arrows indicate the neurons which express both EGFP and CRF. III, third ventricle. Scale bars = 100 μm (25 μm for inset).

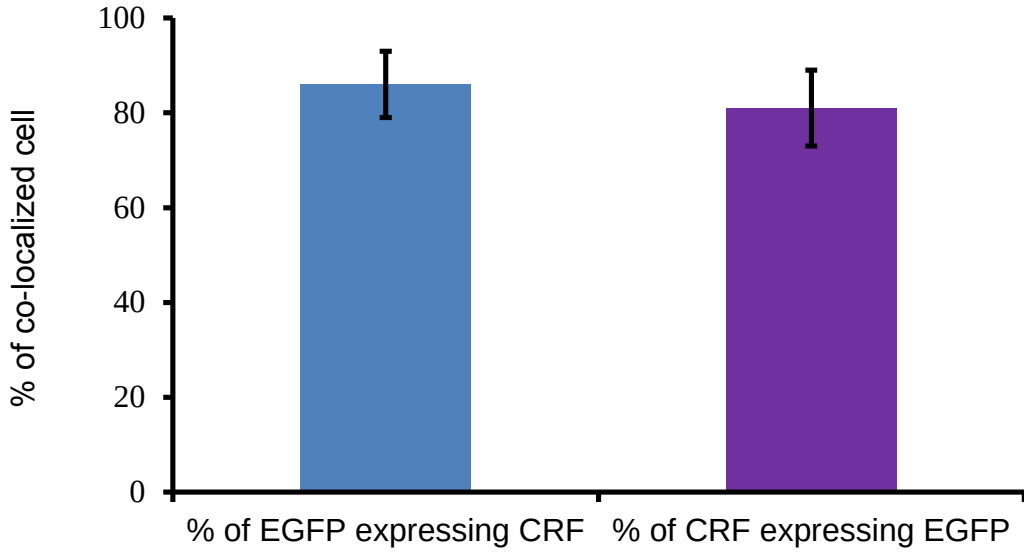

Figure 6: Percentage of EGFP cells that express CRF and vice versa in the PVH of *EGFP/CRF-iCre* mouse. Values are mean ± SEM, n = 3.

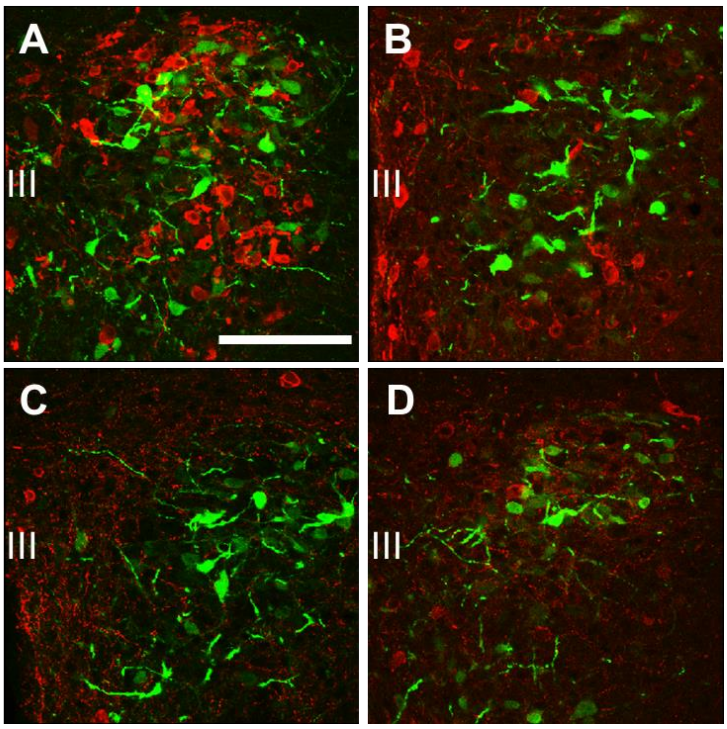

Figure 7: Double immunohistochemistry was carried out to examine whether the Venus-expressing neurons co-express vasopressin (AVP) (A), oxytocin (OXT) (B), somatostatin (SRIF) (C), or thyrotropin-releasing hormone (TRH) (D) in the PVH of naive colchicine-treated *CRF-Venus* mice; representative dual confocal photomicrographs are shown. The Venus neurons did not express OXT, SRIF, or TRH. They were also devoid of AVP expression, with very few exceptions. Venus is colored green, AVP, OXT, SRIF, and TRH red. III, the side of the third ventricle. Scale bar = 100 μm.

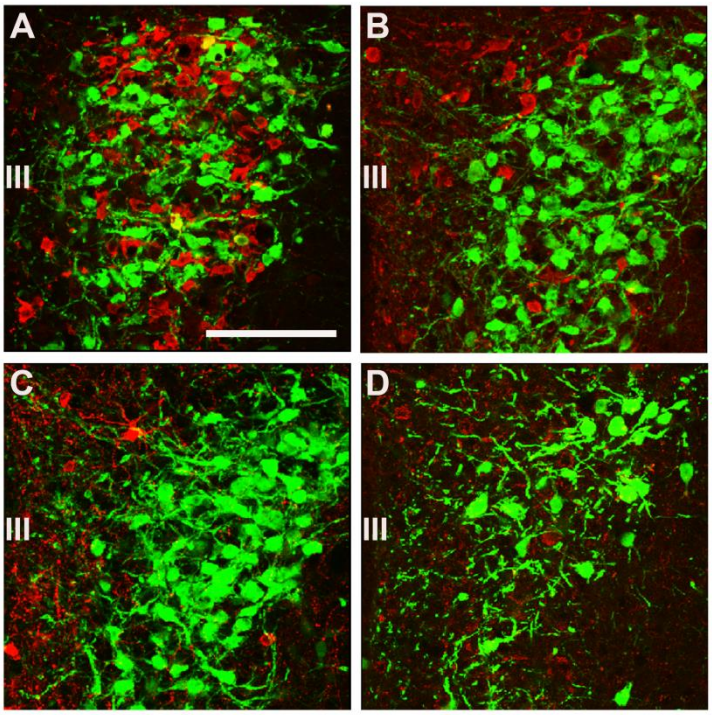

Figure 8: Double immunohistochemistry was carried out to examine whether the EGFP-expressing neurons co-express vasopressin (AVP) (A), oxytocin (OXT) (B), somatostatin (SRIF) (C), or thyrotropin-releasing hormone (TRH) (D) in the PVH of naive colchicine-treated *EGFP/CRF-iCre* mice; representative dual confocal photomicrographs are shown. The EGFP neurons did not express OXT, SRIF, or TRH. They were also devoid of AVP expression, with very few exceptions. EGFP is colored green, AVP, OXT, SRIF, and TRH red. III, the side of the third ventricle. Scale bar = 100 μm.

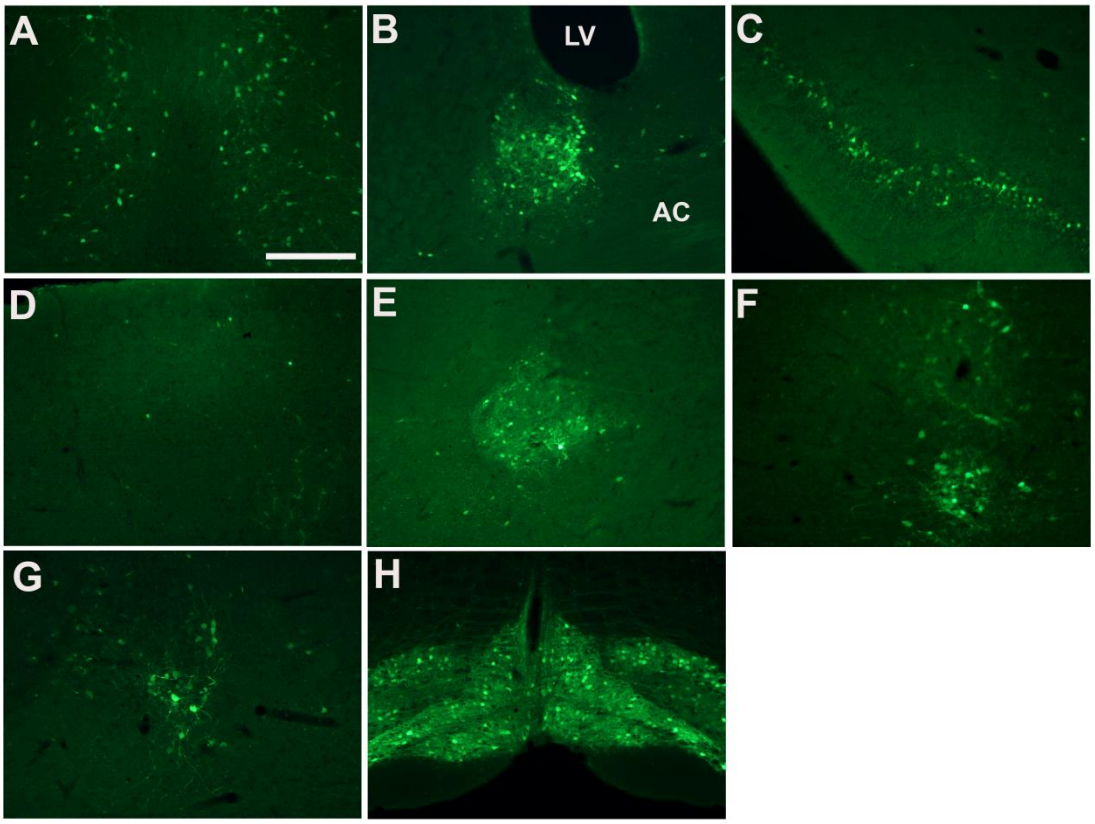

Figure 9: Representative photomicrographs of Venus-expressing neurons in the outside of PVH of colchicine treated naive *CRF-Venus* brain are shown in A-H. Distribution of Venus neurons was examined by single immunohistochemistry. Medial preoptic area (A), dorsal bed nucleus of stria terminalis (B), piriform cortex (C), sensory motor cortex (D), central nucleus of the amygdala (E), laterodorsal tegmental nucleus (F), Barrington's nucleus (G), and inferior olivary nucleus (H). LV, lateral ventricle, AC, anterior commissure, IV, fourth ventricle. Scale bar = 250 μm.

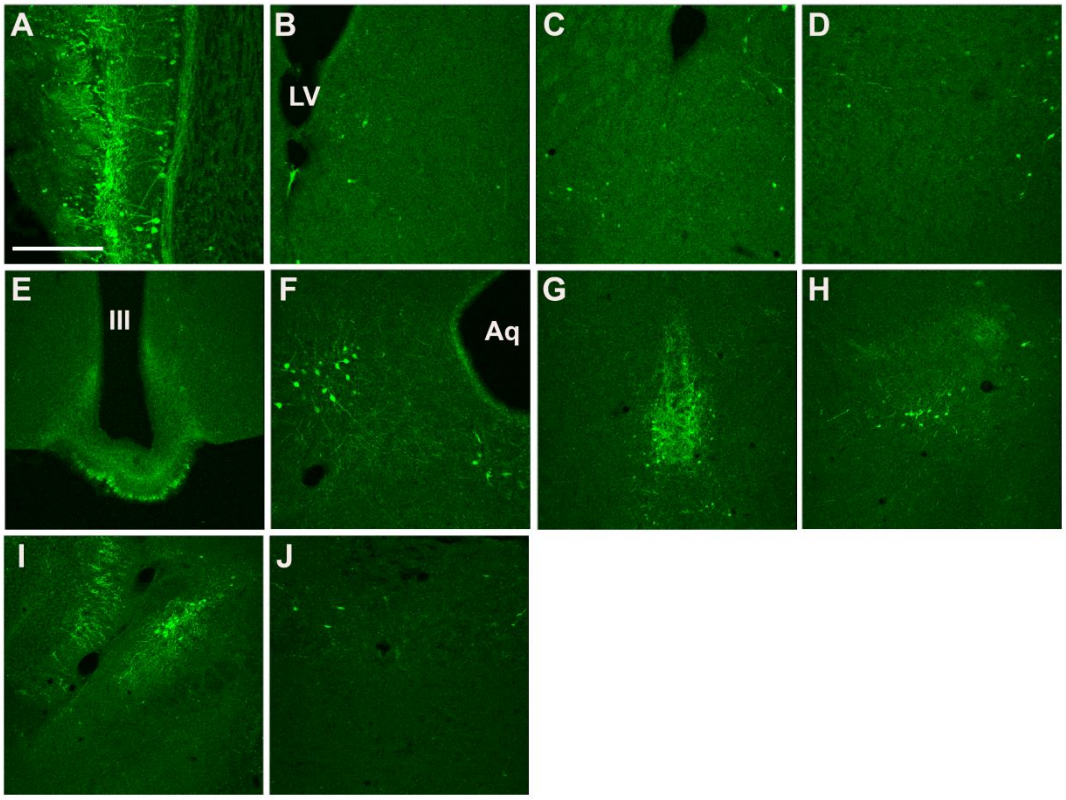

Figure 10: Representative photomicrographs of Venus-expressing neurons in the outside of PVH of colchicine treated naive *CRF-Venus* brain are shown in A-J. Distribution of Venus neurons was examined by single immunohistochemistry. Olfactory tubercle (A), lateral septum (B), accumbens nucleus (C), lateral hypothalamus (D), median eminence (E), periaqueductal gray (F), median raphe nucleus (G), peduncular pontine tegmental nucleus (H), lateral parabrachial nucleus (I), and nucleus of the solitary tract (J). LV, lateral ventricle, Aq, aqueduct, III, third ventricle. Scale bar = 250 μm.

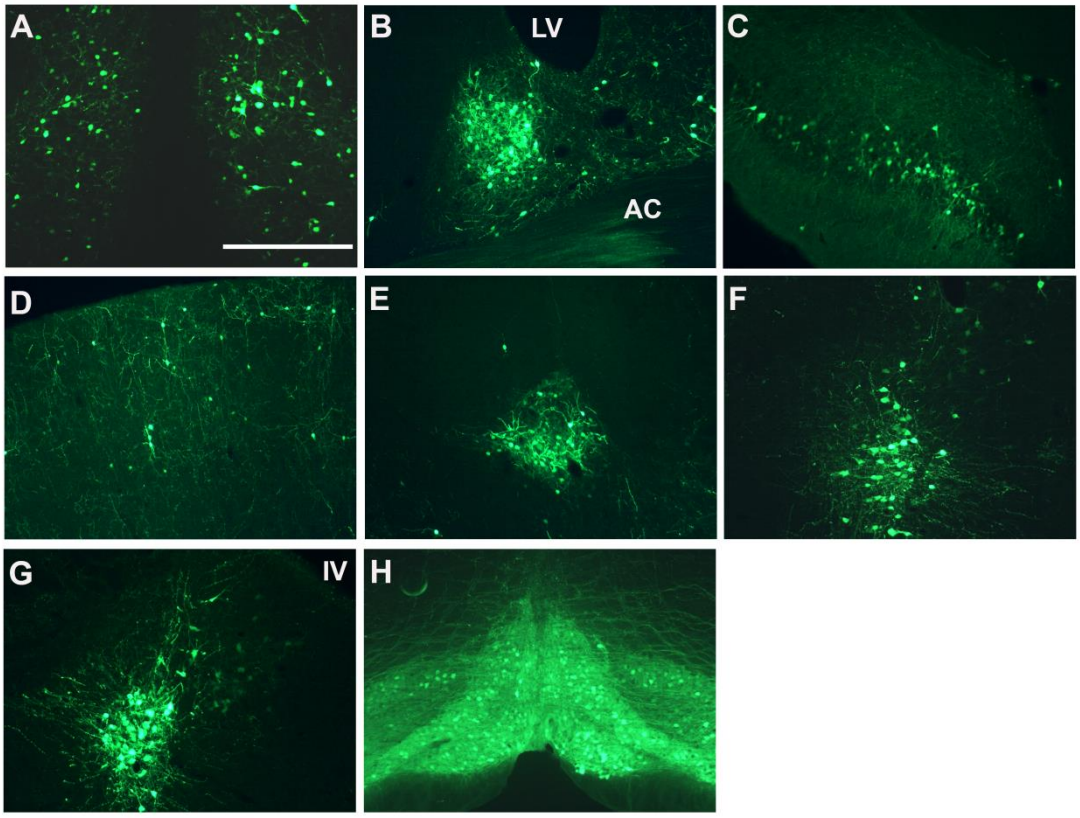

Figure 11: Representative photomicrographs of Venus-expressing neurons in the outside of PVH of colchicine treated naive *CRF-VenusΔneo* mouse brain are shown in A-H. Distribution of Venus neurons was examined by single immunohistochemistry. Medial preoptic area (A), bed nucleus of stria terminalis (B), piriform cortex (C), sensory motor cortex (D), central nucleus of the amygdala (E), laterodorsal tegmental nucleus (F), Barrington's nucleus (G), and inferior olivary nucleus (H). LV, lateral ventricle, AC, anterior commissure, IV, fourth ventricle. Scale bar = 250 μm.

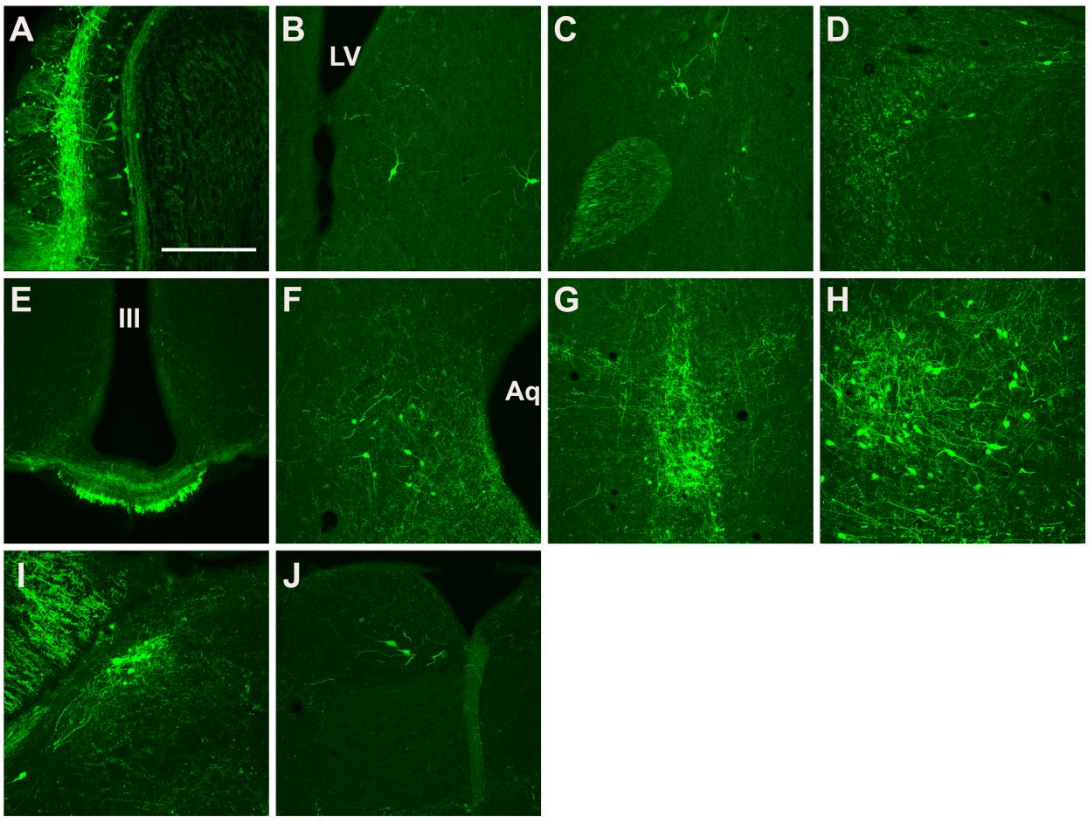

Figure 12: Representative photomicrographs of Venus-expressing neurons in the outside of PVH of colchicine treated naive *CRF-VenusΔneo* brain are shown in A-J. Distribution of Venus neurons was examined by single immunohistochemistry. Olfactory tubercle (A), lateral septum (B), accumbens nucleus (C), lateral hypothalamus (D), median eminence (E), periaqueductal gray (F), median raphe nucleus (G), peduncular pontine tegmental nucleus (H), lateral parabrachial nucleus (I), and nucleus of the solitary tract (J). LV, lateral ventricle, Aq, aqueduct, III, third ventricle. Scale bar = 250 μm.

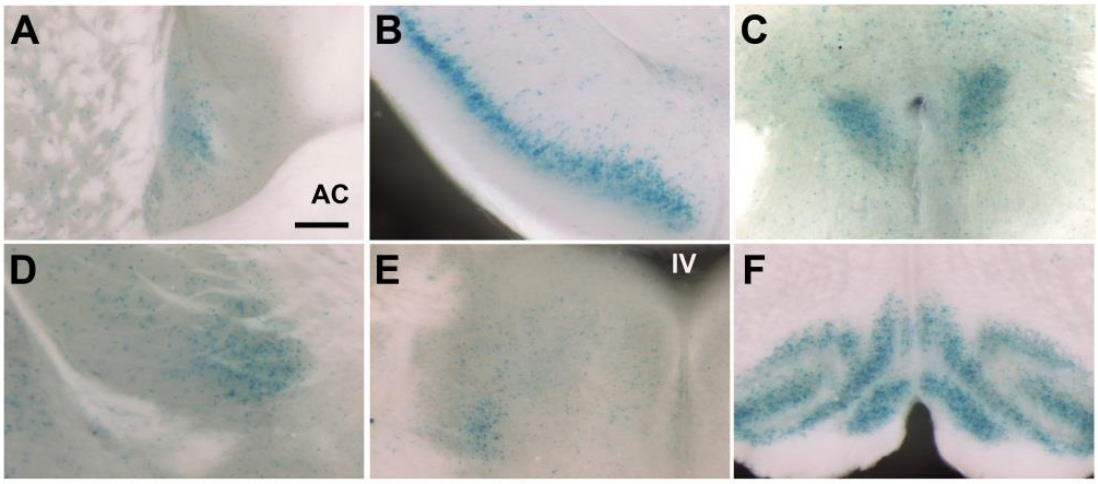

Figure 13: Representative photomicrographs of β-galactosidase-expressing neurons in the *Z/CRF-iCre* brain in (A-F). β-galactosidase neurons examined by X-gal staining. Bed nucleus of stria terminalis (A), piriform cortex (B), paraventricular nucleus (C), central nucleus of the amygdala (D), Barrington's nucleus (E), and inferior olivary nucleus (F). AC, anterior commissure, IV, fourth ventricle. Scale bar = 250 μm.

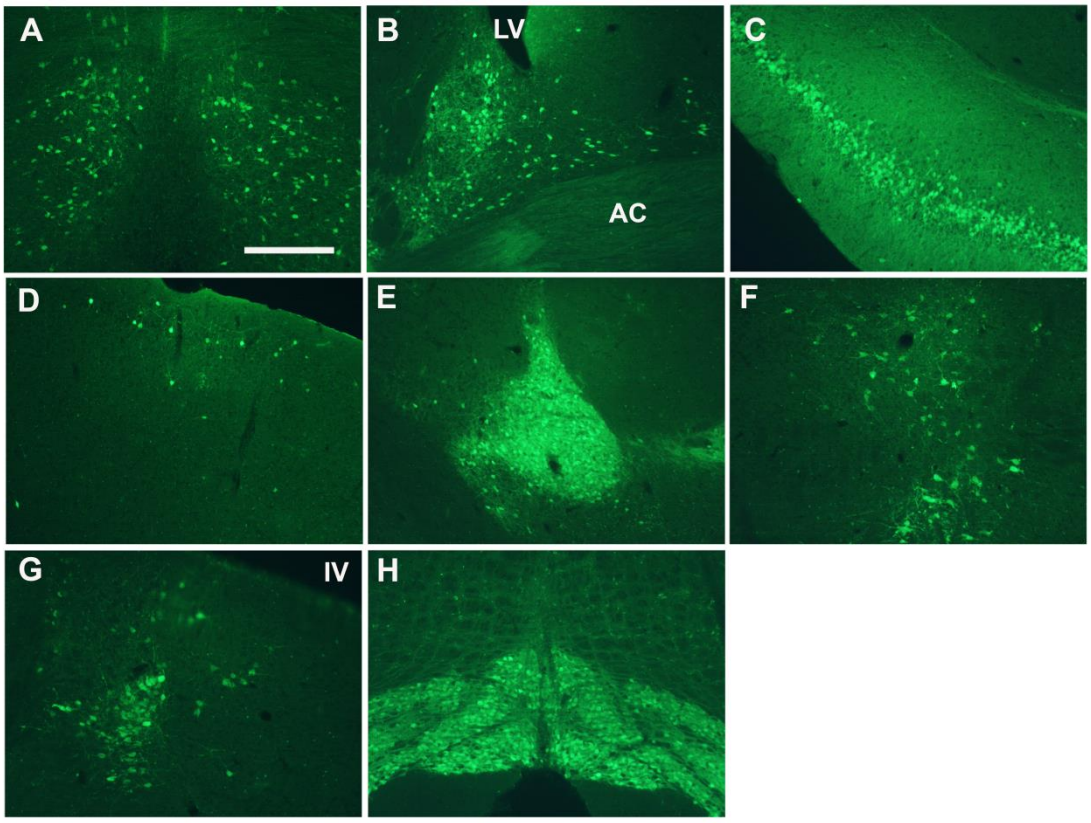

Figure 14: Representative photomicrographs of EGFP-expressing neurons in the outside of PVH of colchicine treated naive *EGFP/CRF-iCre* brain are shown in A-H. Distribution of EGFP neurons was examined by single immunohistochemistry. Medial preoptic area (A), bed nucleus of stria terminalis (B), piriform cortex (C), sensory motor cortex (D), central nucleus of the amygdala (E), laterodorsal tegmental nucleus (F), Barrington's nucleus (G), and inferior olivary nucleus (H). LV, lateral ventricle, AC, anterior commissure, IV, fourth ventricle. Scale bar = 250 μm.

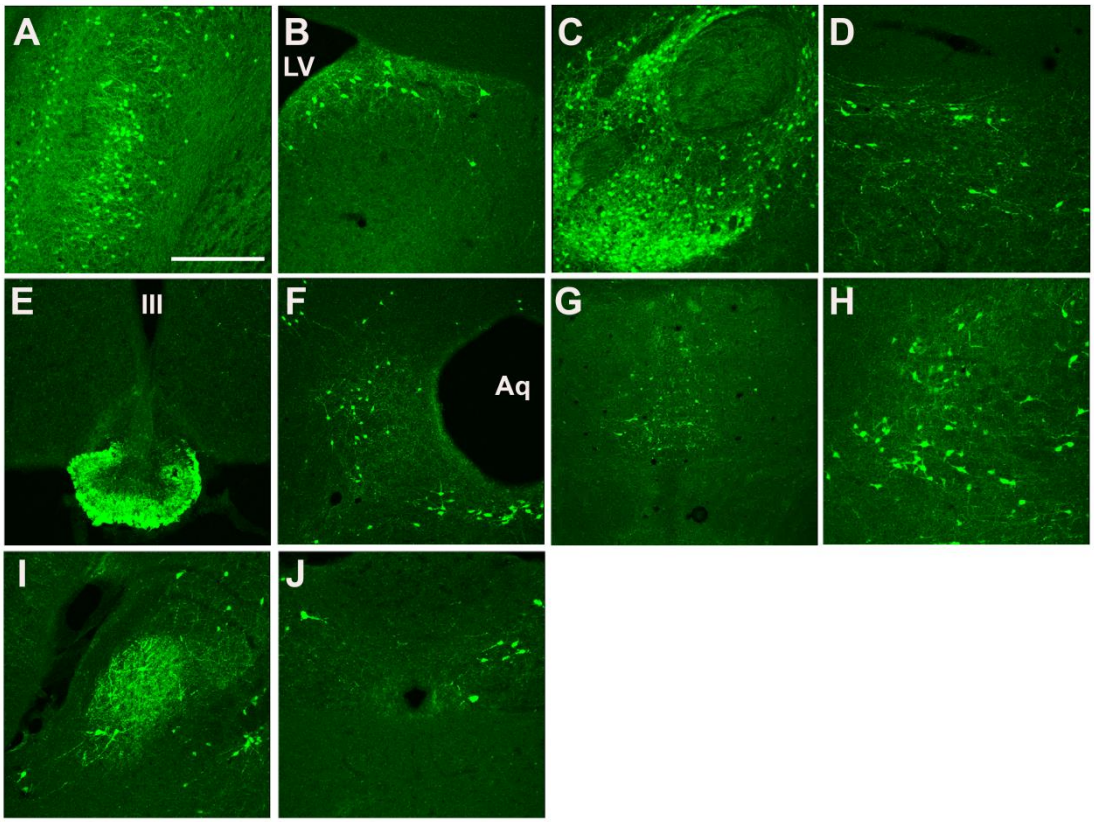

Figure 15: Representative photomicrographs of EGFP-expressing neurons in the outside of PVH of colchicine treated naive *EGFP/CRF-iCre* brain are shown in A-J. Distribution of EGFP neurons was examined by single immunohistochemistry. Olfactory tubercle (A), lateral septum (B), accumbens nucleus (C), lateral hypothalamus (D), median eminence (E), periaqueductal gray (F), median raphe nucleus (G), peduncular pontine tegmental nucleus (H), lateral parabrachial nucleus (I), and nucleus of the solitary tract (J). LV, lateral ventricle, Aq, aqueduct, III, third ventricle. Scale bar = 250 μm.

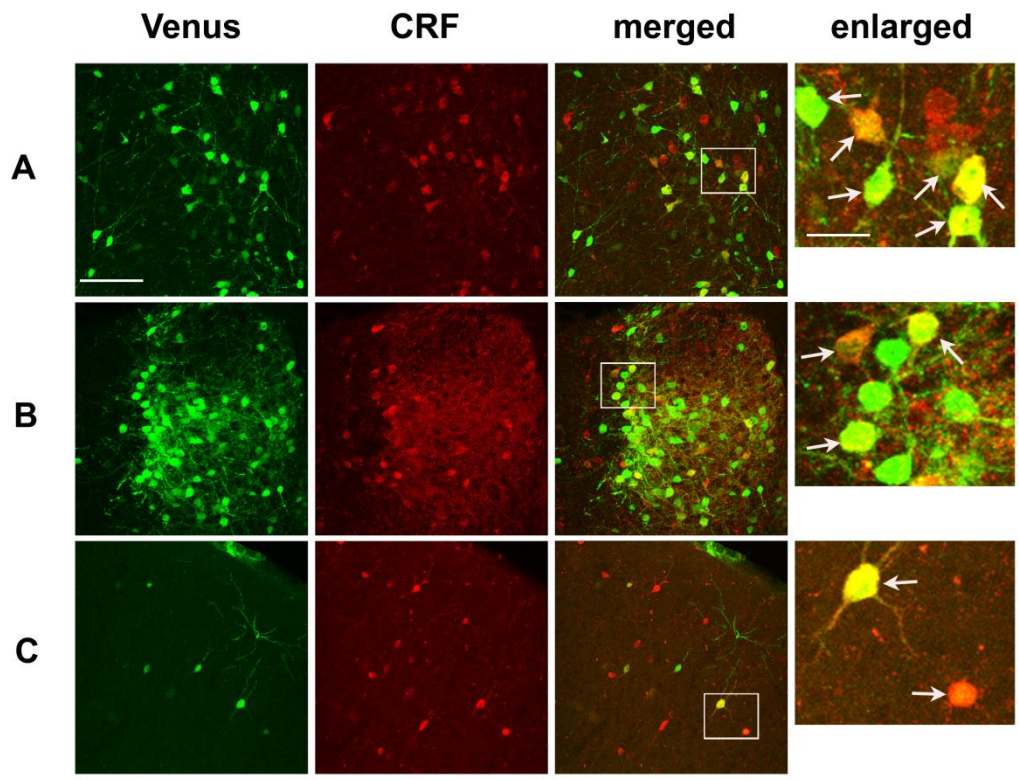

Figure 16: Photomicrographs representing distribution of Venus-expressing neurons (green), CRF-expressing neurons (red) and merged view in the medial preoptic area (A row), dorsal bed nucleus of stria terminalis (B row), and sensory motor cortex (C row) of colchicine treated naive *CRF-Venus* mouse. Enlarged: circumscribed areas are shown in a higher magnification at the right side of each photomicrograph. Arrows indicate the neurons which express both Venus and CRF. Scale bars = 100 μm (25 μm for insets).

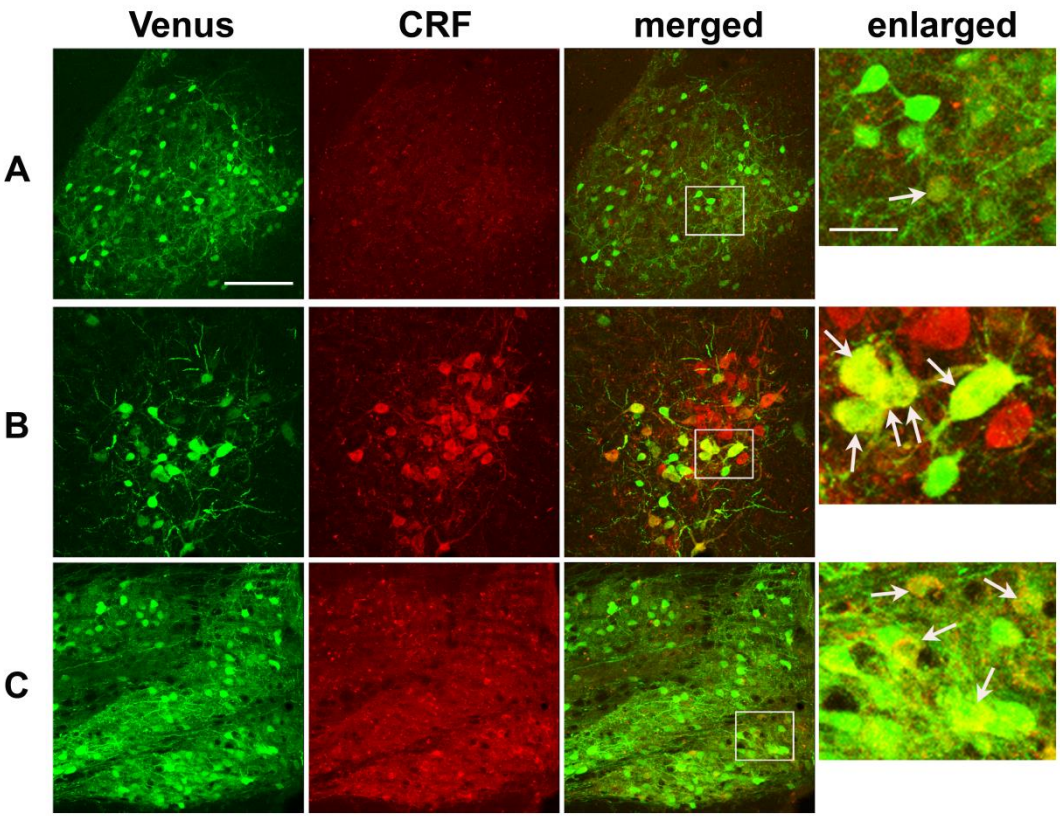

Figure 17: Photomicrographs representing distribution of Venus-expressing neurons (green), CRF-expressing neurons (red) and merged view in the central nucleus of amygdala (A row), Barrington's nucleus (B row), and inferior olivary nucleus (C row) of colchicine treated naive *CRF-Venus* mouse. Enlarged: circumscribed areas are shown in a higher magnification at the right side of each photomicrograph. Arrows indicate the neurons which express both Venus and CRF. Scale bars = 100 μm (25 μm for insets).

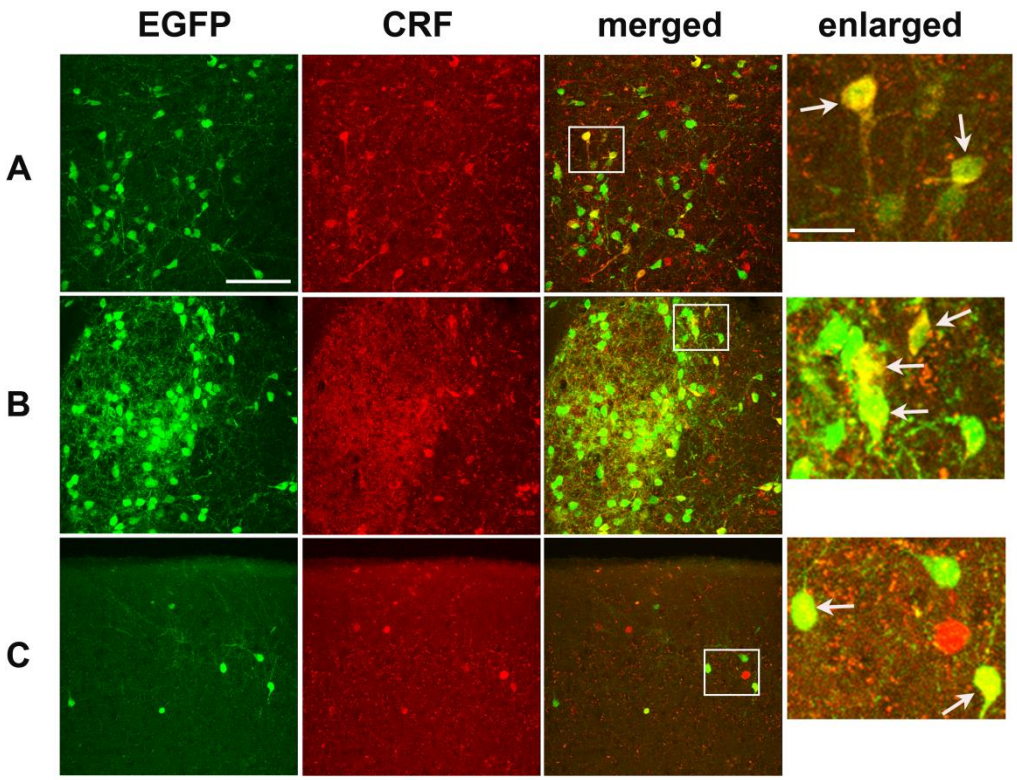

Figure 18: Photomicrographs representing distribution of EGFP-expressing neurons (green), CRF-expressing neurons (red) and merged view in the medial preoptic area (A row), dorsal bed nucleus of stria terminalis (B row), and sensory motor cortex (C row) of colchicine treated naive EGFP/*CRF-iCre* mouse. Enlarged: circumscribed areas are shown in a higher magnification at the right side of each photomicrograph. Arrows indicate the neurons which express both Venus and CRF. Scale bars = 100 μm (25 μm for insets).

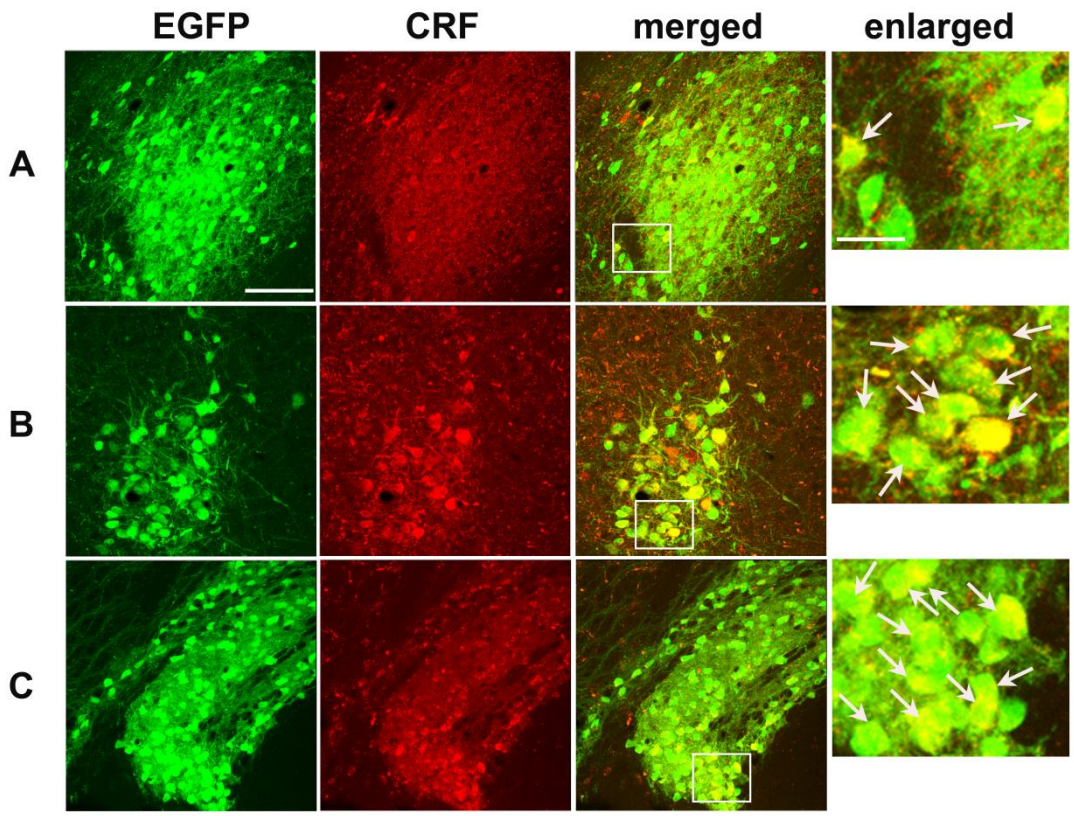

Figure 19: Photomicrographs representing distribution of EGFP-expressing neurons (green), CRF-expressing neurons (red) and merged view in the central nucleus of amygdala (A row), Barrington's nucleus (B row), and inferior olivary nucleus (C row) of colchicine treated naive EGFP/*CRF-iCre* mouse. Enlarged: circumscribed areas are shown in a higher magnification at the right side of each photomicrograph. Arrows indicate the neurons which express both Venus and CRF. Scale bars = 100 μm (25 μm for insets).

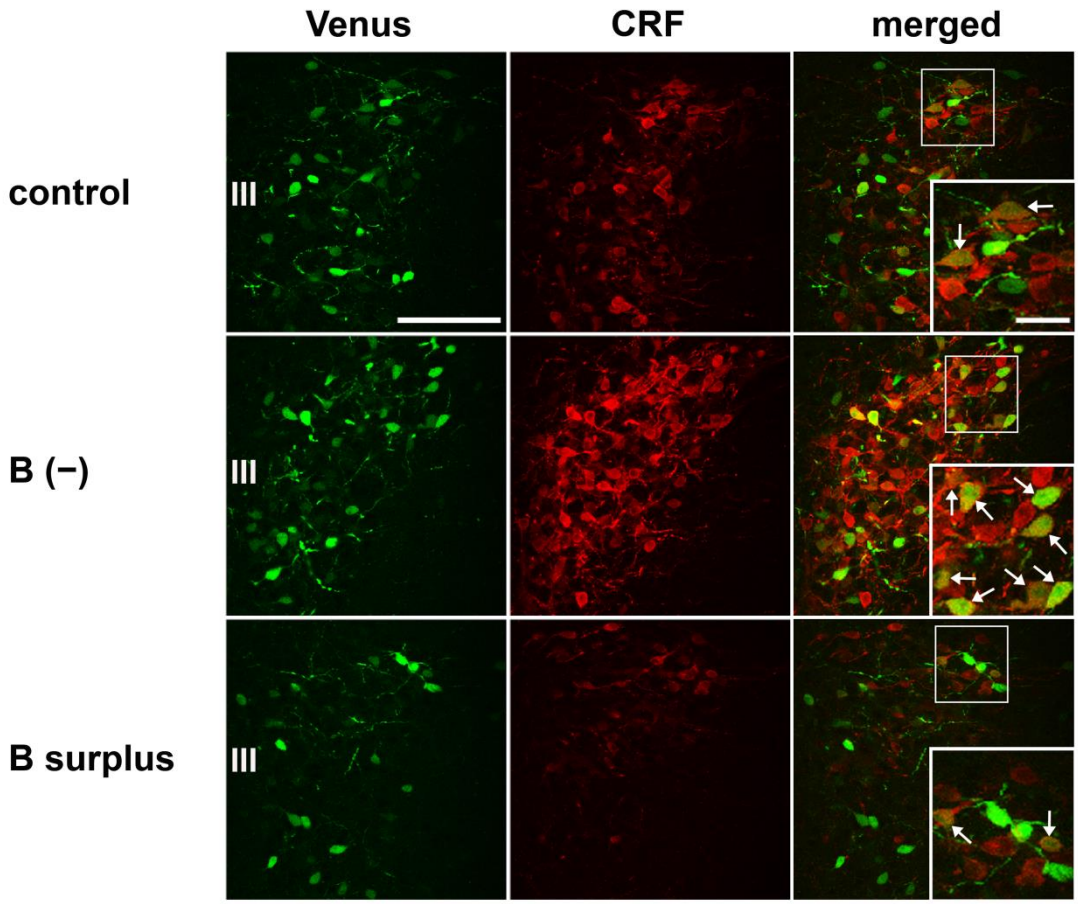

Figure 20: Photomicrographs representing distribution of Venus-expressing neurons (green) and CRF-expressing neurons (red) in the PVH of different group of *CRF-Venus* mouse. Control, sham-operated mouse; B (−), B-deprived mouse; B surplus, mouse given excess B continuously after ADX. Insets: circumscribed areas are shown in a higher magnification at the right lower angle of each photomicrograph. Arrows indicate the neurons which express both Venus and CRF. III, third ventricle. Scale bars = 100 μm (25 μm for insets).

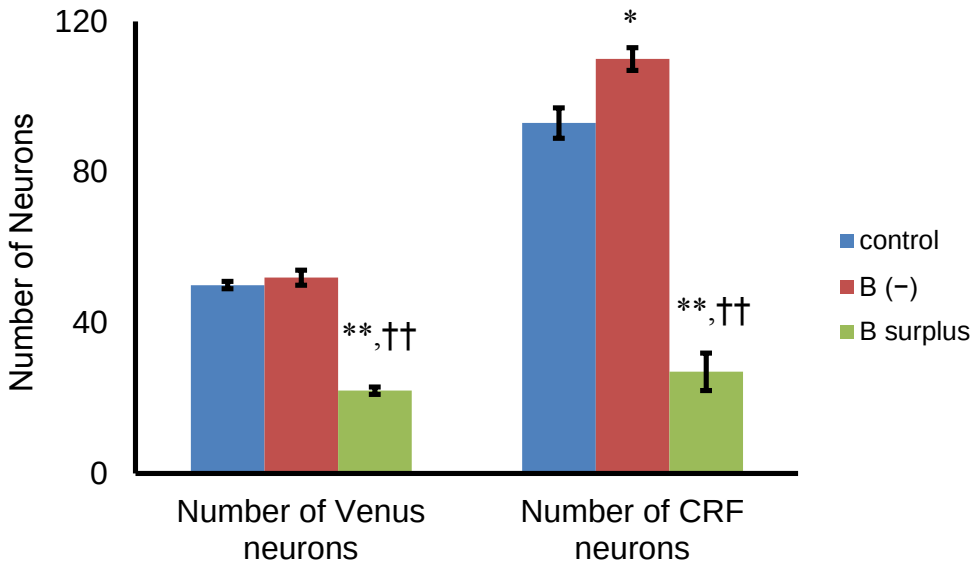

Figure 21: Number of Venus and CRF neurons per unilateral PVH in the different group of *CRF-Venus* mouse. Control, sham-operated mouse; B (−), B-deprived mouse; B surplus, mouse given excess B continuously after ADX. Values are mean ± SEM. *, $P < 0.05$, **, $P < 0.01$ vs. control; †, $P < 0.05$, ††, $P < 0.01$ vs. B (−); ANOVA followed by Tukey's *post-hoc* test. n = 4 per group.

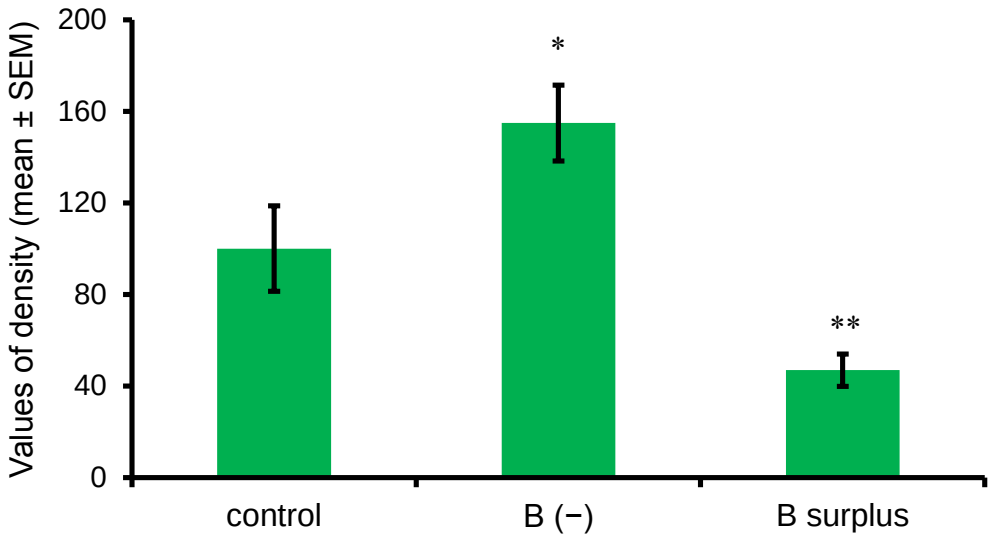

Figure 22: Intensity of Venus neurons per unilateral PVH in the different group of *CRF-Venus* mouse. Control, sham-operated mouse; B (−), B-deprived mouse; B surplus, mouse given excess B continuously after ADX. The mean of the integrated density values (mean density × area) for control normalized into 100 and compare with the values for B (−) and B surplus. *, $P < 0.05$, **, $P < 0.01$ vs. control; Paired t-test. n = 4 per group.

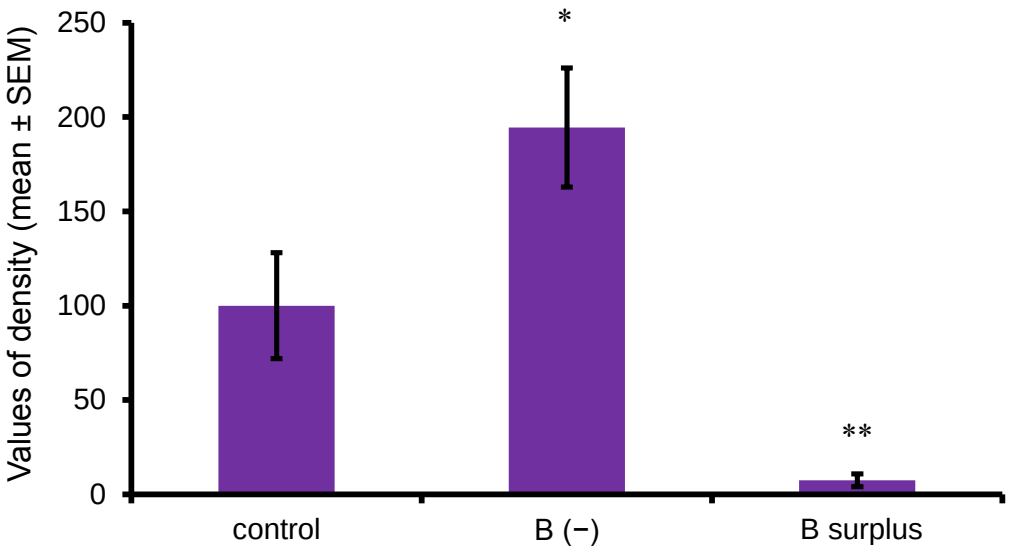

Figure 23: Intensity of CRF neurons per unilateral PVH in the different group of *CRF-Venus* mouse. Control, sham-operated mouse; B (−), B-deprived mouse; B surplus, mouse given surplus B continuously after ADX. The mean of the integrated density values (mean density × area) for control normalized into 100 and compare with the values for B (−) and B surplus. *, $P < 0.05$, **, $P < 0.01$ vs. control; Paired t-test. n = 4 per group.

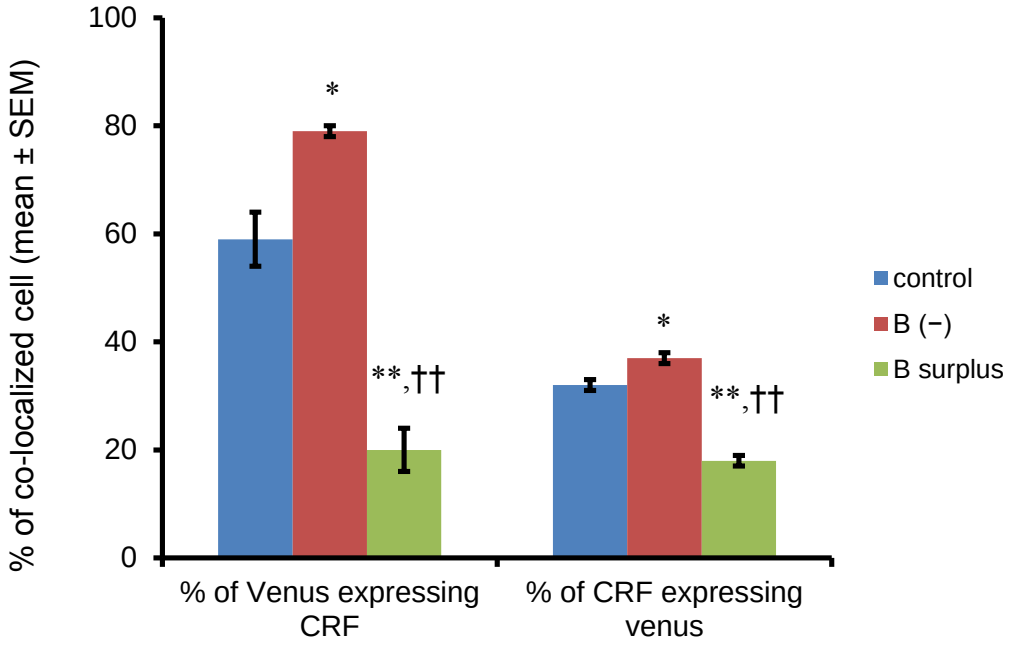

Figure 24: Percentage of Venus cell that express CRF and vice versa in the PVH of different group of *CRF-Venus* mouse. Control, sham-operated mouse; B (−), B-deprived mouse; B surplus, mouse given excess B continuously after ADX. *, $P < 0.05$, **, $P < 0.01$ vs. control; †, $P < 0.05$, ††, $P < 0.01$ vs. B (−); ANOVA followed by Tukey's *post-hoc* test. n = 4 per group.

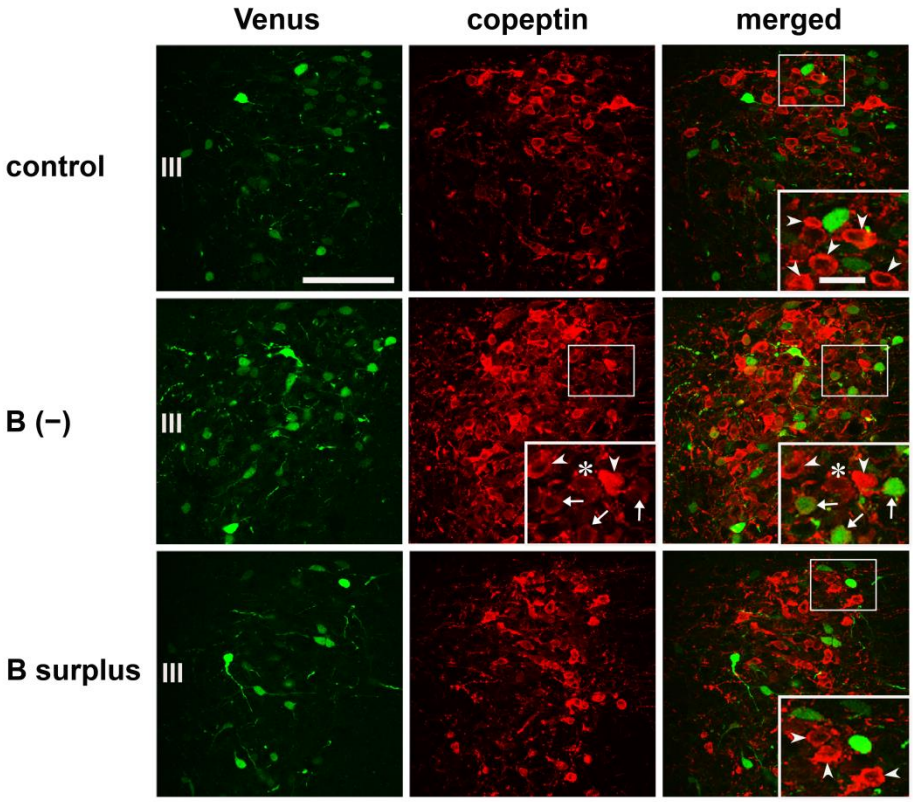

Figure 25: Comparative distribution of Venus-expressing neurons to that of copeptin-expressing neurons in the PVH of the different group of *CRF-Venus* mouse. Control, sham-operated mouse; B (−), B-deprived mouse; B surplus, mouse given surplus B continuously after ADX. Insets: circumscribed areas are shown in a higher magnification at the right lower angle of each photomicrograph. In a majority of the Venus/copeptin expressing neurons, the copeptin expression was of lower intensity (*arrows*), but high-intensity copeptin neurons predominated among those without Venus expression (*arrowheads*) although low-intensity ones were also present (*asterisk*). III, the side facing the third ventricle. Scale bar = 100 μm (25 μm for insets).

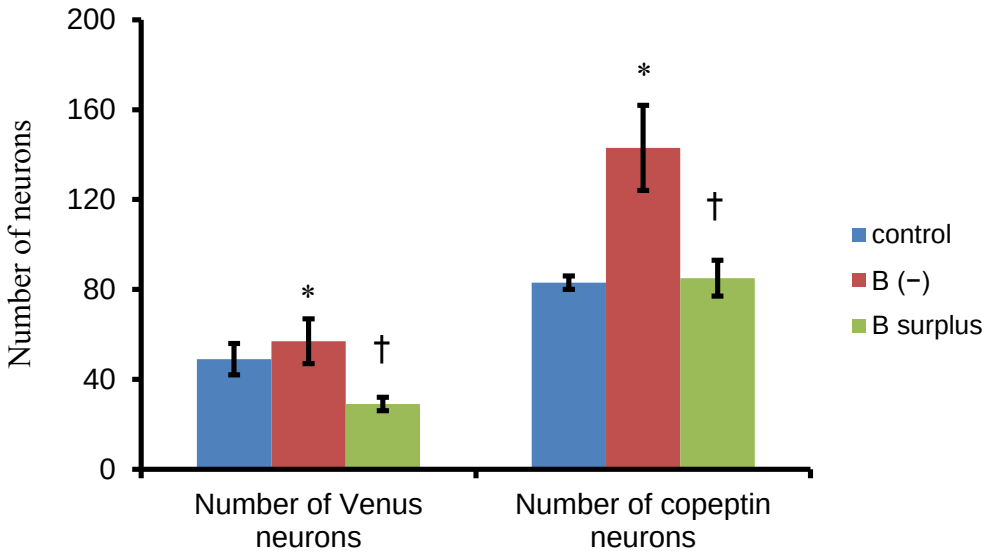

Figure 26: Number of Venus and copeptin (Vasopressin) neurons per unilateral PVH in the different group of *CRF-Venus* mouse. Control, sham-operated mouse; B (−), B-deprived mouse; B surplus, mouse given surplus B continuously after ADX. Values are mean ± SEM. *, $P < 0.05$ vs. control; †, $P < 0.05$ vs. B (−); ANOVA followed by Tukey's *post-hoc* test. n = 4 per group.

.

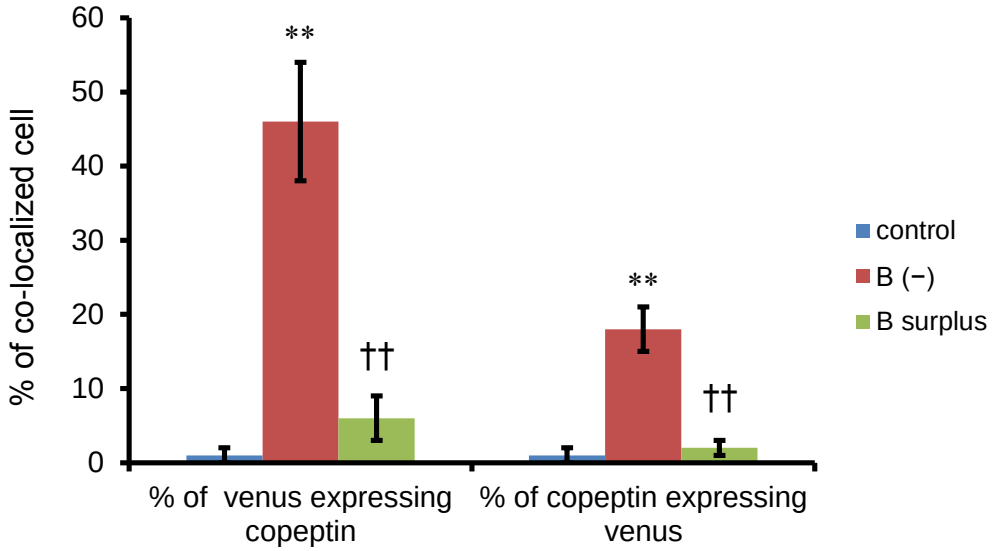

Figure 27: Percentage of Venus cells that express copeptin and vice versa in the PVH of different group of CRF-Venus mouse. Control, sham-operated mouse; B (−), B-deprived mouse; B surplus, mouse given surplus B continuously after ADX. Values are mean ± SEM. **, $P < 0.01$ vs. control; ††, $P < 0.01$ vs. B (−); ANOVA followed by Tukey's *post-hoc* test. n = 4 per group.

Summary

1. In all mouse lines, Venus or EGFP was expressed in most brain regions which are known to express CRF.
2. In the PVH of *CRF-Venus* mouse, colocalization ratio of Venus with CRF was related to the circulating glucocorticoid levels: this is probably because Venus is under the control of CRF promoter.
3. In the PVH of *CRF-Venus*Δ*neo* mouse, Venus was expressed prominently and the number was similar to the number of CRF neuron, and mostly Venus neuron expressed CRF and vice versa.
4. In the PVH of *EGFP/CRF-iCre* mouse, most CRF neurons expressed EGFP, and vice versa, whether or not it underwent ADX: this is probably because EGFP is expressed under the CAG promoter.
5. At physiological stage, the PVH-Venus or EGFP cells were devoid of SRIF, TRH, OXY and almost devoid of AVP confirming the selectivity of Venus or EGFP expression in CRF neurons.
6. Majority of Venus neurons expressed copeptin (vasopressin) following B deprivation in the PVH of *CRF-Venus* mouse, which was not observed in mice either sham operated or given high dose of B continuously. This is recapitulating the characteristics of CRF neurons whose AVP expression is highly dependent on glucocorticoid levels.

Conclusion

In this study a novel mouse line, *CRF-Venus*, is presented. The genomic construct of the mouse was designed so that the Venus expression is driven by CRF promoter. As was demonstrated in the present study, Venus expression in the PVH was strictly dependent upon the GC state of the animal. This may be an advantage in monitoring the dynamic changes in CRF neurons and CRF networks during different GC states, including high GC state and GC deficiency. *CRF-VenusΔneo* mouse also presented in which Venus expressed more constitutively, and Venus expression is also driven by CRF promoter but detail study is required to demonstrate this mouse line.

On the other hand, *EGFP/CRF-iCre* and the mouse reported by Wamsteeker Cusulin and colleagues may have an advantage in labeling CRF neurons more constitutively. Therefore, each mouse model may preferably be chosen depending upon the aim of the study.

References

1. Itoi K, Jiang YQ, Iwasaki Y, Watson SJ: **Regulatory mechanisms of corticotropin-releasing hormone and vasopressin gene expression in the hypothalamus**. *J Neuroendocrinol* 2004, **16**(4):348-355.

2. Aguilera G: **HPA axis responsiveness to stress: implications for healthy aging**. *Exp Gerontol*, **46**(2-3):90-95.

3. Vale W, Spiess J, Rivier C, Rivier J: **Characterization of a 41-residue ovine hypothalamic peptide that stimulates secretion of corticotropin and beta-endorphin**. *Science* 1981, **213**(4514):1394-1397.

4. Sakanaka M, Shibasaki T, Lederis K: **Corticotropin releasing factor-like immunoreactivity in the rat brain as revealed by a modified cobalt-glucose oxidase-diaminobenzidine method**. *J Comp Neurol* 1987, **260**:256-298.

5. Merchenthaler I: **Corticotropin releasing factor (CRF)-like immunoreactivity in the rat central nervous system. Extrahypothalamic distribution**. *Peptides* 1984, **5 Suppl 1**:53-69.

6. GABRY KE, CHROUSOS G, GOLD PW: **The hypothalamic-pituitary-adrenal (HPA) axis: A major mediator of the adaptive responses to stress**. *NeuroImmune Biology* 2003, **3**:379-414.

7. Zorrilla EP, Reinhardt LE, Valdez GR, Inoue K, Rivier JE, Vale WW, Koob GF: **Human urocortin 2, a corticotropin-releasing factor (CRF)2 agonist, and ovine CRF, a CRF1 agonist, differentially alter feeding and motor activity**. *J Pharmacol Exp Ther* 2004, **310**(3):1027-1034.

8. Kovacs KJ: **CRH: the link between hormonal-, metabolic- and behavioral responses to stress**. *J Chem Neuroanat*, **54**:25-33.

9. Wood SK, McFadden K, Griffin T, Wolfe JH, Zderic S, Valentino RJ: **A corticotropin-releasing factor receptor antagonist improves urodynamic dysfunction produced by social stress or partial bladder outlet obstruction in**

male rats. *Am J Physiol Regul Integr Comp Physiol*, **304**(11):R940-950.

10. Wang XD, Labermaier C, Holsboer F, Wurst W, Deussing JM, Muller MB, Schmidt MV: **Early-life stress-induced anxiety-related behavior in adult mice partially requires forebrain corticotropin-releasing hormone receptor 1**. *Eur J Neurosci*, **36**(3):2360-2367.

11. Ito M: **Functional roles of neuropeptides in cerebellar circuits**. *Neuroscience* 2009, **162**(3):666-672.

12. Itoi K, Sugimoto N: **The brainstem noradrenergic systems in stress, anxiety and depression**. *J Neuroendocrinol*, **22**(5):355-361.

13. Itoi K, Suda T, Tozawa F, Dobashi I, Ohmori N, Sakai Y, Abe K, Demura H: **Microinjection of norepinephrine into the paraventricular nucleus of the hypothalamus stimulates corticotropin-releasing factor gene expression in conscious rats**. *Endocrinology* 1994, **135**(5):2177-2182.

14. Itoi K, Helmreich DL, Lopez-Figueroa MO, Watson SJ: **Differential regulation of corticotropin-releasing hormone and vasopressin gene transcription in the hypothalamus by norepinephrine**. *J Neurosci* 1999, **19**(13):5464-5472.

15. Levy BH, Tasker JG: **Synaptic regulation of the hypothalamic-pituitary-adrenal axis and its modulation by glucocorticoids and stress**. *Front Cell Neurosci*, **6**:24.

16. Fuzesi T, Wittmann G, Liposits Z, Lechan RM, Fekete C: **Contribution of noradrenergic and adrenergic cell groups of the brainstem and agouti-related protein-synthesizing neurons of the arcuate nucleus to neuropeptide-y innervation of corticotropin-releasing hormone neurons in hypothalamic paraventricular nucleus of the rat**. *Endocrinology* 2007, **148**(11):5442-5450.

17. Uchoa ET, Aguilera G, Herman JP, Fiedler JL, Deak T, de Sousa MB: **Novel aspects of glucocorticoid actions**. *J Neuroendocrinol*.

18. Kawata M, Hashimoto K, Takahara J, Sano Y: **Differences in the distributional pattern of CRF-, oxytocin-, and vasopressin-immunoreactive nerve fibers in the median eminence of the rat**. *Cell Tissue Res* 1983, **230**(2):247-258.

19. Antoni FA, Kovacs KJ, Dohanits J, Makara GB, Holmes MC, Mazurek MF: **Hypophysiotrophic function of vasopressin and oxytocin**. *Brain Res Bull* 1988, **20**(6):729-736.

20. Aguilera G, Liu Y: **The molecular physiology of CRH neurons**. *Front Neuroendocrinol*, **33**(1):67-84.

21. Itoi K, Seasholtz AF, Watson SJ: **Cellular and extracellular regulatory mechanisms of hypothalamic corticotropin-releasing hormone neurons**. *Endocr J* 1998, **45**(1):13-33.

22. Das G, Uchida K, Kageyama K, Iwasaki Y, Suda T, Itoi K: **Glucocorticoid dependency of surgical stress-induced FosB/DeltaFosB expression in the paraventricular and supraoptic nuclei of the rat hypothalamus**. *J Neuroendocrinol* 2009, **21**(10):822-831.

23. Watts AG: **Glucocorticoid regulation of peptide genes in neuroendocrine CRH neurons: a complexity beyond negative feedback**. *Front Neuroendocrinol* 2005, **26**(3-4):109-130.

24. Itoi K, Mouri T, Takahashi K, Murakami O, Imai Y, Sasaki S, Yoshinaga K, Sasano N: **Suppression by glucocorticoid of the immunoreactivity of corticotropin-releasing factor and vasopressin in the paraventricular nucleus of rat hypothalamus**. *Neurosci Lett* 1987, **73**(3):231-236.

25. de Souza LM, Franci CR: **Differential immunoreactivity of glucocorticoid receptors and vasopressin in neurons of the anterior and medial parvocellular subdvisions of the hypothalamic paraventricular nucleus**. *Brain Res Bull*, **82**(5-6):271-278.

26. Kiss JZ, Mezey E, Skirboll L: **Corticotropin-releasing factor-immunoreactive neurons of the paraventricular nucleus become vasopressin positive after adrenalectomy**. *Proc Natl Acad Sci U S A* 1984, **81**(6):1854-1858.

27. Swanson LW, Sawchenko PE, Rivier J, Vale WW: **Organization of ovine corticotropin-releasing factor immunoreactive cells and fibers in the rat brain: an immunohistochemical study**. *Neuroendocrinology* 1983, **36**(3):165-186.

28. Wamsteeker Cusulin JI, Fuzesi T, Watts AG, Bains JS: **Characterization of corticotropin-releasing hormone neurons in the paraventricular nucleus of the hypothalamus of Crh-IRES-Cre mutant mice**. *PLoS One*, **8**(5):e64943.

29. Alon T, Zhou L, Perez CA, Garfield AS, Friedman JM, Heisler LK: **Transgenic mice expressing green fluorescent protein under the control of the corticotropin-releasing hormone promoter**. *Endocrinology* 2009, **150**(12):5626-5632.

30. Madisen L, Zwingman TA, Sunkin SM, Oh SW, Zariwala HA, Gu H, Ng LL, Palmiter RD, Hawrylycz MJ, Jones AR *et al*: **A robust and high-throughput Cre reporting and characterization system for the whole mouse brain**. *Nat Neurosci*, **13**(1):133-140.

31. Mishina M, Sakimura K: **Conditional gene targeting on the pure C57BL/6 genetic background**. *Neurosci Res* 2007, **58**(2):105-112.

32. Fukaya M, Tsujita M, Yamazaki M, Kushiya E, Abe M, Akashi K, Natsume R, Kano M, Kamiya H, Watanabe M *et al*: **Abundant distribution of TARP gamma-8 in synaptic and extrasynaptic surface of hippocampal neurons and its major role in AMPA receptor expression on spines and dendrites**. *Eur J Neurosci* 2006, **24**(8):2177-2190.

33. Sakai K, Miyazaki J: **A transgenic mouse line that retains Cre recombinase activity in mature oocytes irrespective of the cre transgene transmission**. *Biochem Biophys Res Commun* 1997, **237**(2):318-324.

34. Kawamoto S, Niwa H, Tashiro F, Sano S, Kondoh G, Takeda J, Tabayashi K, Miyazaki J: **A novel reporter mouse strain that expresses enhanced green fluorescent protein upon Cre-mediated recombination**. *FEBS Lett* 2000, **470**(3):263-268.

35. Jacobson L, Akana SF, Cascio CS, Scribner K, Shinsako J, Dallman MF: **The adrenocortical system responds slowly to removal of corticosterone in the absence of concurrent stress**. *Endocrinology* 1989, **124**(5):2144-2152.

36. Akana SF, Jacobson L, Cascio CS, Shinsako J, Dallman MF: **Constant corticosterone replacement normalizes basal adrenocorticotropin (ACTH) but**

permits sustained ACTH hypersecretion after stress in adrenalectomized rats. *Endocrinology* 1988, **122**(4):1337-1342.

37. Daikoku S, Okamura Y, Kawano H, Tsuruo Y, Maegawa M, Shibasaki T: **Immunohistochemical study on the development of CRF-containing neurons in the hypothalamus of the rat**. *Cell Tissue Res* 1984, **238**:539-544.

38. Mouri T, Itoi K, Takahashi K, Suda T, Murakami O, Yoshinaga K, Andoh N, Ohtani H, Masuda T, Sasano N: **Colocalization of corticotropin-releasing factor and vasopressin in the paraventricular nucleus of the human hypothalamus**. *Neuroendocrinology* 1993, **57**(1):34-39.

39. Kadar A, Sanchez E, Wittmann G, Singru PS, Fuzesi T, Marsili A, Larsen PR, Liposits Z, Lechan RM, Fekete C: **Distribution of hypophysiotropic thyrotropin-releasing hormone (TRH)-synthesizing neurons in the hypothalamic paraventricular nucleus of the mouse**. *J Comp Neurol*, **518**(19):3948-3961.

40. Rubin AN, Alfonsi F, Humphreys MP, Choi CK, Rocha SF, Kessaris N: **The germinal zones of the basal ganglia but not the septum generate GABAergic interneurons for the cortex**. *J Neurosci*, **30**(36):12050-12062.

41. Takeuchi T, Nomura T, Tsujita M, Suzuki M, Fuse T, Mori H, Mishina M: **Flp recombinase transgenic mice of C57BL/6 strain for conditional gene targeting**. *Biochem Biophys Res Commun* 2002, **293**(3):953-957.

42. Pham CT, MacIvor DM, Hug BA, Heusel JW, Ley TJ: **Long-range disruption of gene expression by a selectable marker cassette**. *Proc Natl Acad Sci U S A* 1996, **93**(23):13090-13095.

43. Olson EN, Arnold HH, Rigby PW, Wold BJ: **Know your neighbors: three phenotypes in null mutants of the myogenic bHLH gene MRF4**. *Cell* 1996, **85**(1):1-4.

44. Fiering S, Epner E, Robinson K, Zhuang Y, Telling A, Hu M, Martin DI, Enver T, Ley TJ, Groudine M: **Targeted deletion of 5'HS2 of the murine beta-globin LCR reveals that it is not essential for proper regulation of the beta-globin locus**. *Genes Dev* 1995, **9**(18):2203-2213.

45. Tamamaki N, Yanagawa Y, Tomioka R, Miyazaki J, Obata K, Kaneko T: **Green fluorescent protein expression and colocalization with calretinin, parvalbumin, and somatostatin in the GAD67-GFP knock-in mouse**. *J Comp Neurol* 2003, **467**(1):60-79.

46. Keegan CE, Herman JP, Karolyi IJ, O'Shea KS, Camper SA, Seasholtz AF: **Differential expression of corticotropin-releasing hormone in developing mouse embryos and adult brain**. *Endocrinology* 1994, **134**(6):2547-2555.

47. Sawchenko PE, Swanson LW, Vale WW: **Corticotropin-releasing factor: co-expression within distinct subsets of oxytocin-, vasopressin-, and neurotensin-immunoreactive neurons in the hypothalamus of the male rat**. *J Neurosci* 1984, **4**(4):1118-1129.

48. Sofroniew MV, Weindl A, Schinko I, Wetzstein R: **The distribution of vasopressin-, oxytocin-, and neurophysin-producing neurons in the guinea pig brain. I. The classical hypothalamo-neurophypophyseal system**. *Cell Tissue Res* 1979, **196**(3):367-384.

49. Guardiola-Diaz HM, Kolinske JS, Gates LH, Seasholtz AF: **Negative glucorticoid regulation of cyclic adenosine 3', 5'-monophosphate-stimulated corticotropin-releasing hormone-reporter expression in AtT-20 cells**. *Mol Endocrinol* 1996, **10**(3):317-329.

50. Jeanneteau FD, Lambert WM, Ismaili N, Bath KG, Lee FS, Garabedian MJ, Chao MV: **BDNF and glucocorticoids regulate corticotrophin-releasing hormone (CRH) homeostasis in the hypothalamus**. *Proc Natl Acad Sci U S A*, **109**(4):1305-1310.

51. Watts AG: **The impact of physiological stimuli on the expression of corticotropin-releasing hormone (CRH) and other neuropeptide genes**. *Front Neuroendocrinol* 1996, **17**(3):281-326.

52. Bartanusz V, Jezova D, Bertini LT, Tilders FJ, Aubry JM, Kiss JZ: **Stress-induced increase in vasopressin and corticotropin-releasing factor expression in hypophysiotrophic paraventricular neurons**. *Endocrinology* 1993, **132**(2):895-902.

53. Helmreich DL, Itoi K, Lopez-Figueroa MO, Akil H, Watson SJ: **Norepinephrine-induced CRH and AVP gene transcription within the hypothalamus: differential regulation by corticosterone**. *Brain Res Mol Brain Res* 2001, **88**(1-2):62-73.

54. Ueta Y, Dayanithi G, Fujihara H: **Hypothalamic vasopressin response to stress and various physiological stimuli: visualization in transgenic animal models**. *Horm Behav*, **59**(2):221-226.

Acknowledgement

I express my gratitude in the most humble way to almighty Allah.

I have the honor to express my heartfelt thanks and deepest sense of gratitude to my honorable supervisor Dr. Keiichi Itoi, Professor of Information Biology, Graduate School of Information Sciences (GSIS), Tohoku University, and an enormous debt of gratitude for accepting me as a Ph.D. student in his laboratory. I again express my gratitude and indebtedness to my reverend supervisor for his scholarly supervision, instruction, valuable suggestions, encouragement, unprecedented patience and sympathy during the whole period of research works as well as insightful comments on the manuscripts.

I want to express my gratitude to Dr. Katsuya Uchida and Dr. Tohimitsue Fuse, Assistant Professors, Laboratory of Information Biology, GSIS, and Dr. Gopal Das (former postdoctoral fellow) for their technical assistance, valuable suggestions and all supports during my research work. My grateful thanks are also expressed to all my lab mates in the Laboratory of Information Biology, who supported and encouraged me during my study period.

My grateful thanks to Dr.Tamotsu Shibasaki, Nippon Medical School, for giving anti-CRF antibody, Dr. Csaba Fekete, Hungarian Academy of Sciences, for anti-TRH antibody, Dr. Jun-ichi Miyazaki, Osaka University, for *CAG-CAT-LacZ* and *CAG-CAT-EGFP* mice, Dr. Manabu Abe, Niigata University for giving *Actb-Flp knock-in* mouse and Professor Kenji Sakimura for his nice collaboration to generate *CRF-Venus* mouse.

I am very much grateful to the Government of Japan who supported my all expenses by granting MEXT (Ministry of Education, Culture, Sports, Science and Technology) scholarship during my study period. I also would like to express my cordial thanks to the authority of Mawlana Bhashani Science and Technology University (MBSTU) as granted study leave for me.

Finally my cordial thanks to my parents and other family members for their mental support and encouragement during my study in Japan.